SYNTHESIS OF POLYAMPHOLYTES AND THEIR PHASE SEPARATION WITH ENZYMES

by
Esra Baydar
B.S., Chemistry, Boğaziçi University, 2021

Submitted to the Institute for Graduate Studies in
Science and Engineering in partial fulfillment of
the requirements for the degree of
Master of Science

Graduate Program in Chemistry
Boğaziçi University
2024

ACKNOWLEDGEMENTS

First of all, I would like to express my deepest gratitude to my thesis supervisor Assoc. Prof. Ayşe Başak Kayıtmazer for her guidance, support and encouragement throughout the duration of this research journey. I am profoundly grateful for the opportunity to learn under her mentorship and for her patience and understanding.

I would like to thank my thesis committee: Asst. Prof. Fırat İlker for his endless guidance and support and Asoc.Prof. İlke Anaç Şakır for her guidance about the project and for their valuable time.

I would like to extend my thanks to all members of Kayıtmazer Research Group for their contributions to my scientific background and especially to my lab mates, Sezin. Besides, my deepest thank to Fatma, Ayşenur, Göknil, Halenur, Ayşe Zeyneb, and Nazlıcan for their scientific and mental support for this way.

This project has been supported by TÜBİTAK (The Scientific and Technological Research Council of Türkiye) (Project Code: 121Z816) and Boğaziçi University Research Fund (Grant Number 19342M). This thesis was supported by TÜBİTAK National MSc/MA Scholarship Program 2021/2 (BİDEB 2210-A).

ABSTRACT

SYNTHESIS OF POLYAMPHOLYTES AND THEIR PHASE SEPARATION WITH ENZYMES

Complex coacervation is defined as a liquid-liquid phase separation including two phases, one dilute phase called supernatant and one dense phase called coacervate. Coacervation can be used as an encapsulation method that allows for protection of active substances like enzymes from environmental factors; e.g. pH, salt concentrations and temperature. In this method, although oppositely charged polyelectrolytes are mostly used, study of coacervation involving polyampholytes, which are polyelectrolytes with both positive and negative charges, is essential regarding their mimicry of intrinsically disordered proteins, which also carry oppositely charges on their backbone. The aim of this study is to synthesize hyaluronic acid-based polyampholytes (PA) with different grafting ratios with using 1,4-Diaminobutane dihydrochloride (DN), adipic dihydrazide (ADH) and ethylenediamine dihydrochloride (EDA) via carbodiimide chemistry. To characterize these polyampholytes, ^{1}H-Nuclear Magnetic Resonance (^{1}H-NMR) and Fourier-Transform Infrared (FTIR) spectroscopy were used to examine the chemical structure of the modified HA. Zeta potential experiments were conducted to obtain the isoelectric points (pI) of the polyampholytes. Synthesized polyampholytes were used to encapsulate enzymes with different isoelectric points (pI) like alpha-chymotrypsin (αCT) (pI = 8.76), carbonic anhydrase (CA) (pI = 5.9) and lysozyme (LYS) (pI = 11). Turbidimetric titration experiments with changing pH and NaCl concentration were conducted to determine the range where phase separation takes place at the optimum pH of the selected enzymes.

ÖZET

POLİAMFOLİT SENTEZİ VE ENZİMLERLE FAZ AYRIŞMASI

Kompleks koaservasyon, süpernatant olarak adlandırılan bir seyreltik faz ve koaservat olarak adlandırılan bir yoğun faz olmak üzere iki ayrı faz içeren bir sıvı-sıvı faz ayrımı olarak tanımlanır. Koaservasyon, enzimler gibi aktif maddelerin pH, tuz konsantrasyonları ve sıcaklık gibi çevresel faktörlerden korunmasını sağlayan bir enkapsülasyon yöntemi olarak kullanılabilir. Bu yöntemde çoğunlukla zıt yüklü polielektrolitler kullanılsa da, hem pozitif hem de negatif yüklü polielektrolitler olan poliamfolitleri içeren koaservasyon çalışmaları, omurgalarında zıt yükler taşıyan içsel olarak düzensiz proteinleri taklit etmeleri açısından önemlidir. Bu çalışmanın amacı, karbodiimid kimyası yoluyla 1,4-Diaminobutan dihidroklorür (DN), adipik dihidrazid (ADH) ve etilendiamin dihidroklorür (EDA) kullanarak farklı aşılama oranlarına sahip hiyalüronik asit bazlı poliamfolitler (PA) sentezlemektir. Bu poliamfolitleri karakterize etmek için ^{1}H-Nükleer Manyetik Rezonans (^{1}H-NMR) ve Fourier Dönüşümü Kızılötesi (FTIR) spektroskopisi modifiye HA'nın kimyasal yapısını incelemek için kullanılmıştır. Poliamfolitlerin izoelektrik noktalarını (pI) elde etmek için zeta potansiyeli deneyleri yapılmıştır. Sentezlenen poliamfolitler, alfa-kimotripsin (αCT) (pI = 8.76), karbonik anhidraz (CA) (pI = 5.9) ve lizozim (LYS) (pI = 11) gibi farklı izoelektrik noktalarına (pI) sahip enzimleri kapsüllemek için kullanılmıştır. Seçilen enzimlerin optimum pH'ında faz ayrışmasının gerçekleştiği aralığı belirlemek için pH ve NaCl konsantrasyonu değiştirilerek türbidimetrik titrasyon deneyleri yapılmıştır.

TABLE OF CONTENTS

LIST OF FIGURES

LIST OF TABLES

LIST OF SYMBOLS

cm	Centimeter
cP	Centipoise
g/mol	Gram per mole
kDa	Kilodalton
mg	Milligram
mg/mL	Milligram per milliliter
MHz	Megahertz
mL	Milliliter
mM	Millimolar
mmol	Millimole
mV	Millivolts
M_w	Molecular weight
nm	Nanometer
pI	Isoelectric point
w/v	Weight per volume
α	Alpha
MΩ	Megaohm
μm	Micrometer
μL	Microliter
°C	Degree Celcius
% T	Percent transmittance
100 - % T	Turbidity

LIST OF ACRONYMS/ABBREVIATIONS

AcOH	Acetic acid
ADH	Adipic dihydrazide
BLG	β-lactoglobulin
BSA	Bovine serum albumin
BSA	Bovine serum albumin
CA	Carbonic anhydrase
CD	Circular dichroism
CHI	Chitosan
CMC	(1-cyclohexyl-3-(2-morpholinoethyl
CMCh	Carboxymethyl chitosan
CT	Chymotrypsin
DCC	Dicyclohexyl carbodiimide
DLS	Dynamic light scattering
DMSO	Dimethyl sulfoxide
DN	1,4-Diaminobutane dihydrochloride
DNA	Deoxyribonucleic acid
DS	Degree of substitution
EDA	Ethylenediamine dihydrochloride
EDC	1-Ethyl-3-(3-dimethylaminopropyl) Carbodiimide
EtOH	Ethanol
FTIR	Fourier transform infrared
HA	Hyaluronic acid
HCl	Hydrochloric acid
HOBt	1-Hydroxybenzotriazole
LLPS	Liquid-liquid phase separation
LYS	Lysozyme
MOPS	(3-(N-Morpholino)propanesulfonic acid)
MWCO	Molecular weight cutoff
NaCl	Sodium chloride
NaOH	Sodium hydroxide
NHS	N-Hydroxysuccinimide

NMR	Nuclear Magnetic Resonance
PA	Polyampholytes
PAA	Poly(acrylic acid)
PAH	Poly(allylamine)
PDADMAC	Poly-(diallyldimethylammonium chloride)
PE	Polyelectrolyte
PSS	Poly(sodium 4-styrenesulfonate)
RAFT	Reversible-addition fragmentation chain transfer
RNA	Ribonucleic acid
SDS	Sodium dodecyl sulfate
THF	Tetrahydrofuran
TLC	Thin layer chromatography

1. INTRODUCTION

1.1. Coacervation

Coacervation, which is of type of liquid-liquid phase separation (LLPS), is a technique to produce micro- and nano-sized spherical droplets. Phase separation results in two phases: the bottom phase called coacervate, which was first observed by Bungenberg de Jong (1949), is relatively dense and polymer-rich, while the upper phase, which contains a low-concentration of macroions and a higher volume than the lower phase, is called the supernatant. (Figure 1.1) [1,4].

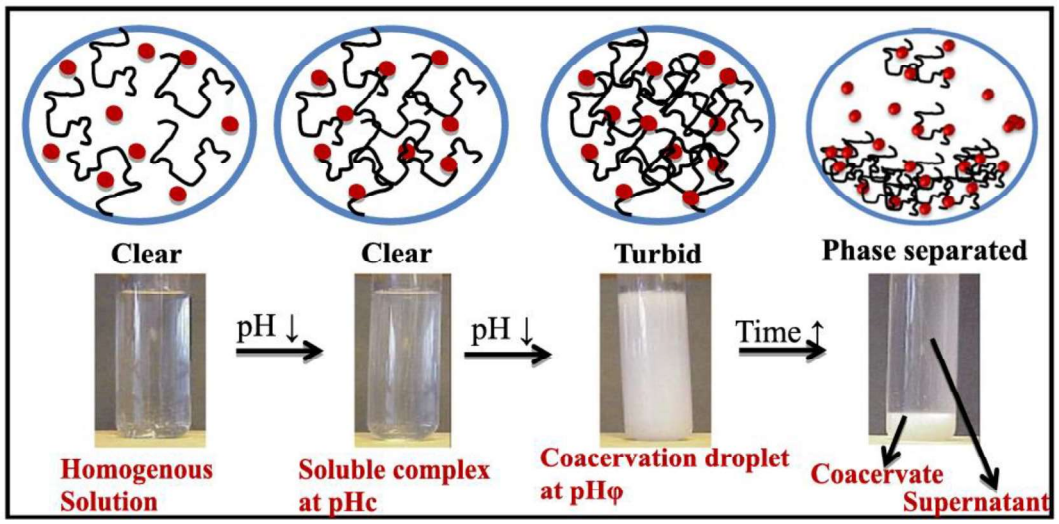

Figure 1.1. Schematic representation of the interaction between proteins and polyelectrolytes (PE) affected by a decrease in pH (Adapted from Ref.[4] with permission from Elsevier)

According to Oparin's theory, there is a strong relationship between the origin of life and coacervates. Oparin emphasized that the droplets of coacervates mimicked protocells due to their similarities like modifiable size, ability of selective absorption and interaction with the environment [5].

Coacervation, which is a self-assembly process, has a wide range of application areas in water treatment [6], purification of proteins [7], food formulation [8] and in pharmaceutical industry as a microencapsulation platform (Figure 1.2) [9,10].

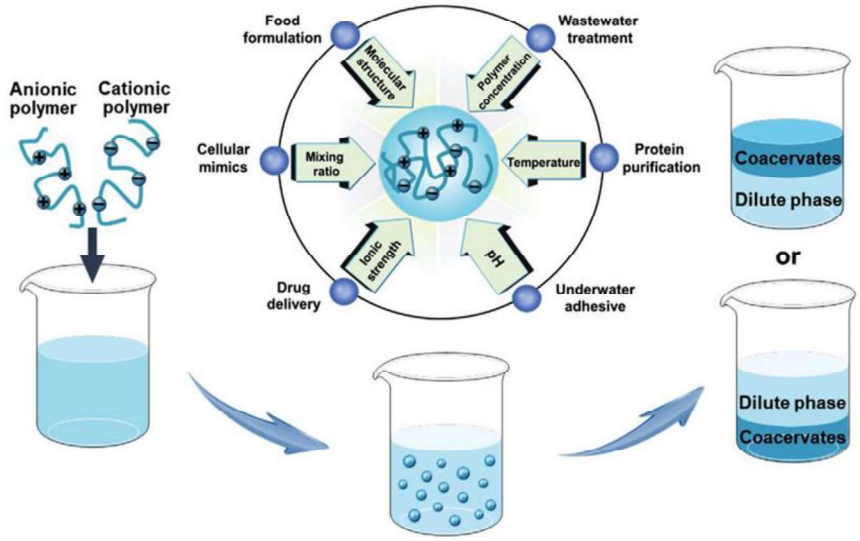

Figure 1.2. Schematic illustration of the parameters that affect the coacervation process and application areas (Reproduced from Ref.[10] from John Wiley and Sons)

There are two types of coacervation, distinguished by the difference in driving forces. One of them is called simple coacervation driven by the hydrophobic interactions formed by dehydrating materials like salt or organic solvents to trigger the desolvation process. For example, Mohanty and Bohidar (2003) obtained simple coacervation by mixing gelatin (type-B) with different types of alcohols like methanol, ethanol, propanol and tert-butyl alcohol while changing the ionic strength from 0.01 M to 0.1 M NaCl [11]. The second type is complex coacervation which is formed by oppositely charged macromolecules or inorganic materials and driven mainly by electrostatic interactions between oppositely charged groups accompanied by entropic forces derived from the releasing of counter-ions. Other than electrostatic interactions, other non-covalent interactions such as hydrogen bonding and hydrophobic interactions can also be used to drive the phase separation [12,13].

Coacervation can be established from bio-based macromolecules such as DNA [14], RNA [15], and polysaccharides [1]. The phenomenon of coacervation has been investigated with respect to various parameters like pH, ionic strength, salt concentration, polymer

concentration, temperature, molecular weight, and charge density. By analyzing how these variables influence the coacervation process, researchers aim to understand the underlying mechanisms and optimize conditions. The effects of these parameters were studied for different systems like polyelectrolyte (PE)-colloid and polyelectrolyte (PE)-polyelectrolyte (PE) mixtures.

Dubin and co-workers investigated phase separation of poly-(diallyldimethylammonium chloride) (PDADMAC), a strong cationic polyelectrolyte, with oppositely charged mixed micelles of Triton X-100 and sodium dodecyl sulfate (SDS) as a model PE-micelle system by changing salt concentrations using turbidimetric titrations [16].

Kayitmazer et al. conducted a study with semi-flexible hyaluronic acid (HA)-chitosan (CHI) biopolymer system to investigate the effect of parameters such as ionic strength, polymer concentration and charge ratio. They conducted turbidimetric titration with salt at different polymer concentrations and observed that increasing salt concentration leads to a screening effect that prevents the interaction between the charged units of the polymers. They observed precipitation with an increase in polymer concentration as a result of the increase in the charges involved in polymer-polymer interactions. In addition, they used light microscopy to observe spherical droplets up to a charge ratio ([-]/[+]) of 0.46, and and precipitates at higher charge ratios [1].

Dubin and co-workers also investigated phase separation of polyelectrolyte (PE) - protein systems using hyaluronic acid (HA), bovine serum albumin (BSA) and β-lactoglobulin (BLG). In that study, in addition to investigating the effect of salt concentration and pH, they also studied on the influence of protein charge anisotropy and net charge of the protein while defining the phase boundaries of phase separation [17].

Aside from phase separation with polyelectrolytes, polyampholytes, which are polymers carrying both negative and positive charges in their repeat unit, are also used for coacervation for innovative developments specifically in synthetic biology and material science. For example, Perro and co-workers used polyacrylic acid and N, N'-dimethyl ethylenediamine to synthesize polyampholytes (PA) with different grafting ratios via carbodiimide chemistry. They accomplished self-coacervation of polyampholytes driven by

the loss of solvency, and focused on the importance of the distribution of negative and positive charges on the same polymer chain [18]. Another example of coacervation with polyampholytes can be given from the study of Muthukumar and co-workers on the interaction between poly (2-methacryloyloxyethyl phosphorylcholine) and poly acrylic acid, where the effects of pH and temperature were investigated as a model polyampholyte-polyelectrolyte [19].

1.2. Polyampholytes

Polyelectrolytes carry either positive or negative charges on their chains. On the other hand, polyampholytes comprise both anionic and cationic monomers which allow them to participate in complex coacervation due to electrostatic interactions. They can be distinguished different types based on their structure and composition, polyampholytes can be mainly classified as random, graft and block polyampholytes [20,21].

This zwitter-ionic structure makes polyampholytes applicable in different areas such as biotechnology [22], material science [23] and pharmaceuticals [24]. The dual-charge mechanism can be used to mimic the membranelles organelles in the context of biological systems [25,26]. Because of the similarity between polyampholytes and proteins, the study of polyampholytes in coacervation systems has gained interest to enlarge the understanding of origin of life [27,28].

Patrickios and co-workers synthesized an ABC triblock methacrylic polyampholyte using group transfer polymerization to investigate its precipitation by changing parameters like pH, salt type and concentration, and presence of a protein. They concluded that precipitation process was favorable around the isoelectric point where the net charge was equal to zero. There was no relation between the polyampholyte concentration and the phase diagram of precipitation but with increasing the salt concentration, the interaction took place at more basic pHs within a narrow pH scale compared to lower salt concentrations. Besides, the isoelectric points of protein (chicken egg lysozyme) and polyampholyte had crucial effects on the pH of coprecipitation [29].

Mirzadeh and coworkers prepared polysaccharide-based polyampholytes of carboxymethyl chitosan (CMCh) [30] using carboxymethyl cellulose and chitosan (CHI) to investigate the differences in complexation between polyampholyte complex (CMCh) system and PE-PA system (CMCh-CHI). They observed that CMCh complex system was more soluble and responsive to ionic strength in contrast to CMCh-CHI system. They attributed their result to the reduced chain spatial conformations because the bulky structure of CMC pave way to less gain in entropy while releasing counter-ions as a consequence. In addition, they pointed out that the weak interaction strength of the PA-complex system was originated from the random charge distribution of polyampholytes, which could be disrupted easily even by small ions like salt [31].

1.2.1. Polyampholyte Synthesis via Carbodiimide Chemistry

There are several methods to synthesize polyampholytes such as free-radical polymerization [32] and reversible-addition fragmentation chain transfer (RAFT) [33]. One of these techniques is based on - carbodiimide chemistry to aminate the main backbone of the polymer chain.

Carbodiimide chemistry is a widely utilized method in peptide synthesis [34] and functionalization of polysaccharides [25]. The usage of carbodiimides has several advantages, two of the most important being composed of non-hazardous reagents and solubility in aqueous medium.

Carbodiimides act as zero-length crosslinker molecules to enable the carboxylate group attach to amine groups to form an amide linkage. Several carbodiimide reagents are frequently used in aqueous or organic mediums, depending on their solubility properties. EDC (1-ethyl-3-(3-dimethylaminopropyl) carbodiimide hydrochloride) and CMC (1-cyclohexyl-3-(2-morpholinoethyl) carbodiimide) are the most common water soluble carbodiimide reagents while DCC (dicyclohexyl carbodiimide) can be used in organic solvents. The water-soluble carbodiimide reagents are employed for biochemical reactions due to the water-soluble characteristics of most biomacromolecules. It should also be emphasized that carbodiimide chemistry enables an easier purification process since not only the main materials but also the side-products of the reaction are dissolved in the same

environment [35]. The general scheme of carbodiimide chemistry is represented in Figure 1.3.

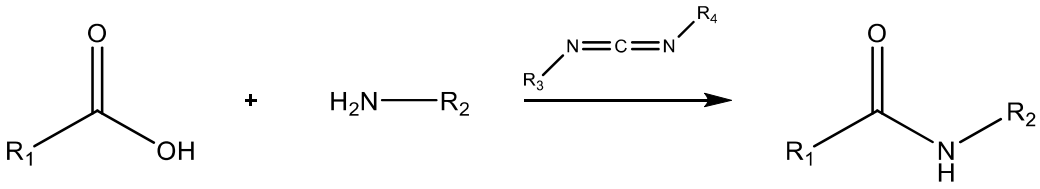

Figure 1.3. The general scheme of carbodiimide chemistry with using primary amine.

Pouyani and Prestwich (1994) employed carbodiimide chemistry to modify carboxyl groups of hyaluronic acid (HA), which is a semi-flexible and biocompatible linear polysaccharide with a repeating unit containing N-acetyl-D-glucosamine and D-glucuronic acid (Figure 1.4.), with amines to conjugate a drug. When aliphatic and aromatic diamines were attempted to modify the carboxylate group of HA at pH 4.75 via EDC, N-acylurea, which was the only product of the reaction, was formed [36].

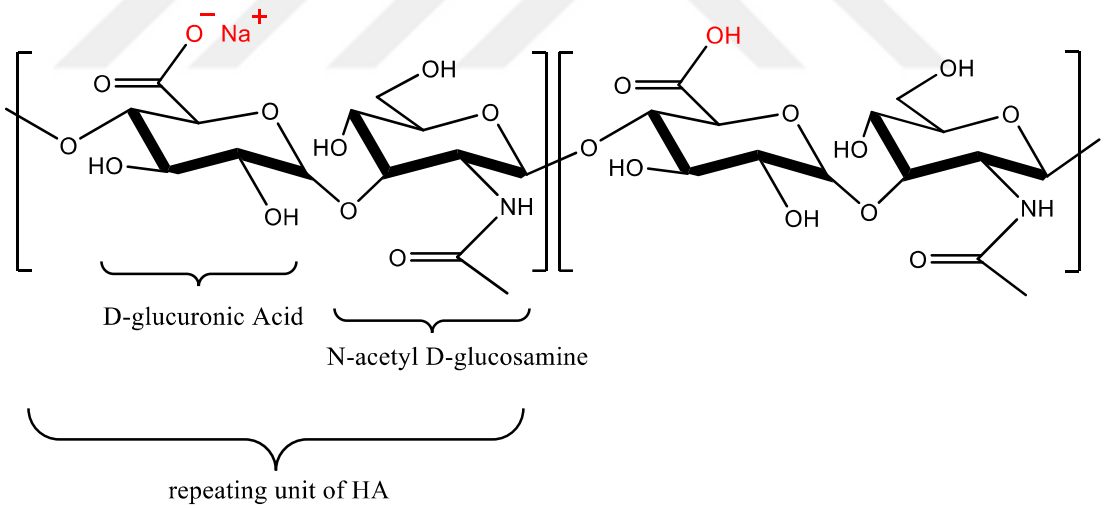

Figure 1.4. Chemical structure of hyaluronic acid (HA).

Nakajima and Ikada (1995) focused on the stability of EDC while investigating amide formation of cyclizable (maleic acid and poly(acrylic acid)) and noncyclizable (fumaric acid and poly(ethylene glycol)) materials. They found that although the activity of EDC decreased sharply at lower pHs in aqueous environment with generation of a urea derivative, EDC stayed active and stable at neutral or more basic pHs. Other outcomes from that study was that (i) carboxylic anhydride formation was needed to obtain an amide bond, and (ii)

cyclizable carboxyl groups had more capability of producing an anhydride rather than noncyclizable ones [37].

Bulpitt and Aeschlimann (1999) focused on coupling HA with amines to obtain hydrogels. Their fundamental challenge was to prevent the formation of N-acylurea, which is a stable and irreversible by-product, and maintain the stability of O-acylisourea so that the latter would go on with amine coupling. For the modification, more basic pH than pH 4.75 was chosen since N-acylurea was formed at the mildly acidic pH 4.75. In addition, they developed a technique to protect O-acylisourea and turn it into an active ester intermediate for the modification of HA with primary amines. For this reason, 1-hydroxybenzotriazole (HOBt) or N-hydroxysulfosuccinimide (sulfo-NHS) was employed depending on the pKa of the selected primary amines [38].

The mechanism of these consecutive reactions that involve HA conjugation with EDC (Figure 1.5) was explained by Mojarradi [39]. In the first step of the amidation reactions, EDC is protonated to form a carbocation. As mentioned above [37], EDC is easily hydrolyzed and becomes inactive by forming a urea derivative at mildly acidic pH (Figure 1.6). When the pH is relatively basic, EDC turns into a carbocation which is attacked by a strong nucleophile, i.e. carboxylate group of HA, to form O-acylisourea (Figure 1.7)

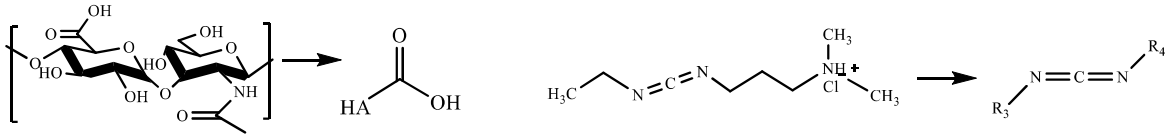

Hyaluronic Acid
(HA)

1-ethyl-3-(3-dimethylaminopropyl) carbodiimide hydrochloride
(EDC)

Figure 1.5. The representations of molecules that are used in the consecutive reaction schemes.

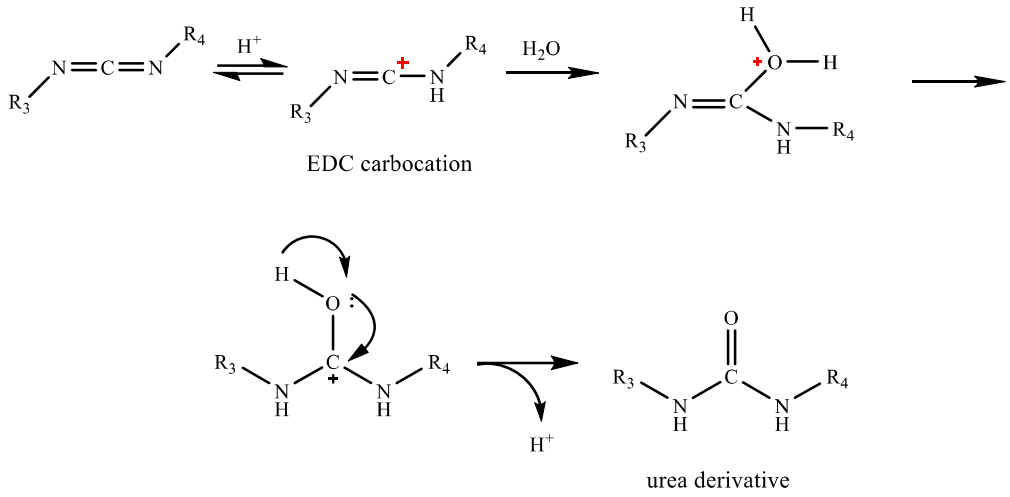

Figure 1.6. The reaction scheme for the formation of an EDC carbocation followed by hydrolysis forming an inactive urea derivative.

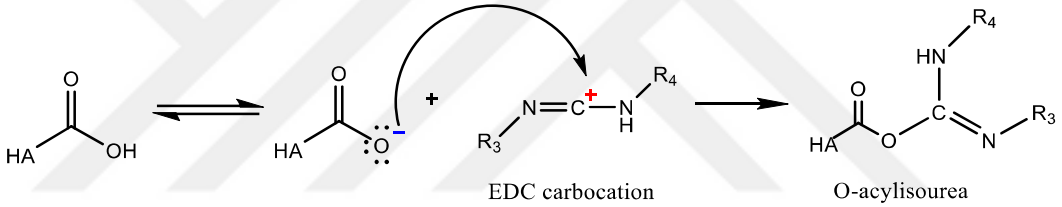

Figure 1.7. The representation of O-acylisourea from EDC carbocation and carboxylate form of HA.

From this point, there are two pathways to obtain an amide bond after O-acylisourea is formed when only EDC is used in the reaction: the first one is that primary amine as a non-dissociated nucleophile can attack the O-acylisourea to form an amide bond by forming a urea-derivative as the side product (Figure 1.8). In the second pathway which is described for cyclizable carboxylate acids by Nakajima and Ikada, an acid anhydride is formed by the attack of carboxylate group of HA, which is also a strong nucleophile, to O-acylisourea (Figure 1.9).

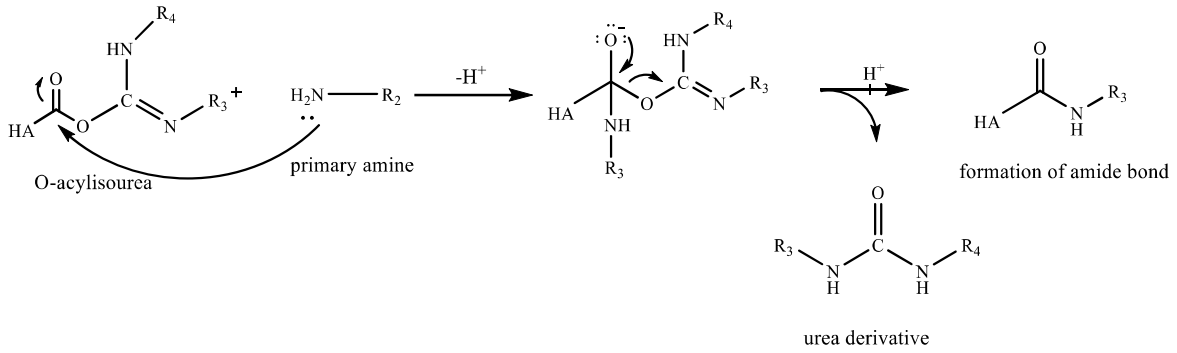

Figure 1.8. The reaction scheme of formation amide bond from O-acylisourea by producing urea side product.

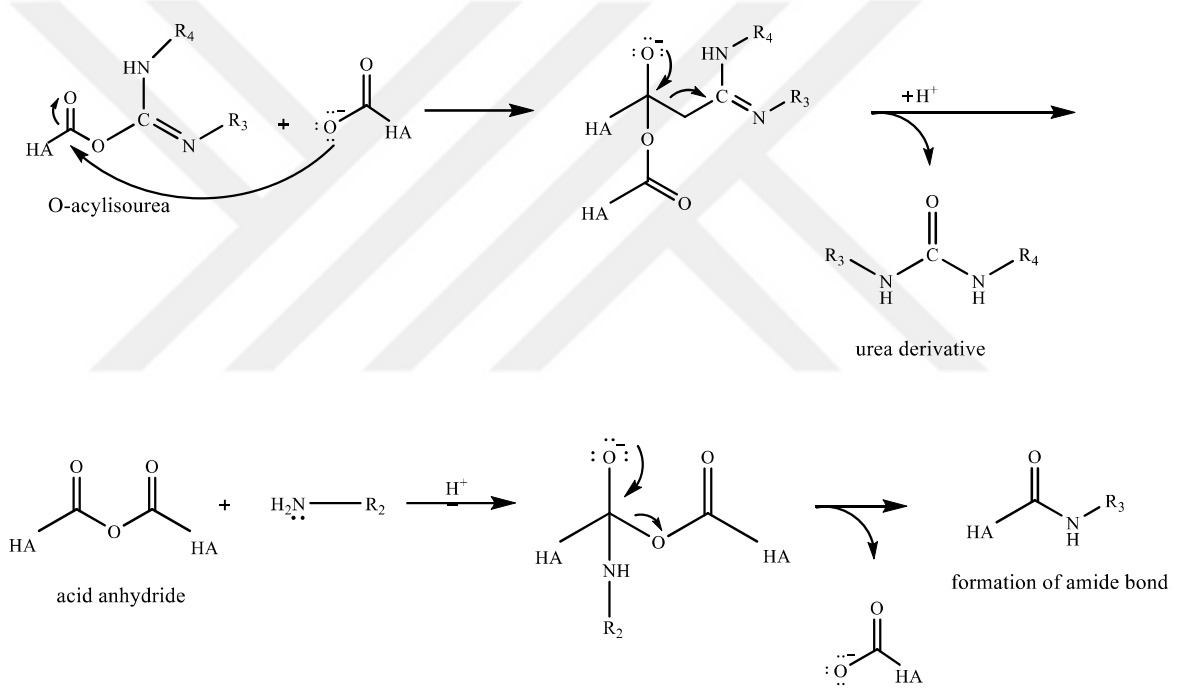

Figure 1.9. The reaction scheme of amide bond formation from acid anhydride via carbodiimide chemistry.

If amide bond is not formed following the formation of O-acylisourea, the reaction can be concluded through two different pathways, one of which is the hydrolysis of O-acylisourea resulting in the formation of a urea derivative and a carboxylate ion derived from HA. The other possibility is the formation of N-acylurea (Figure 1.10).

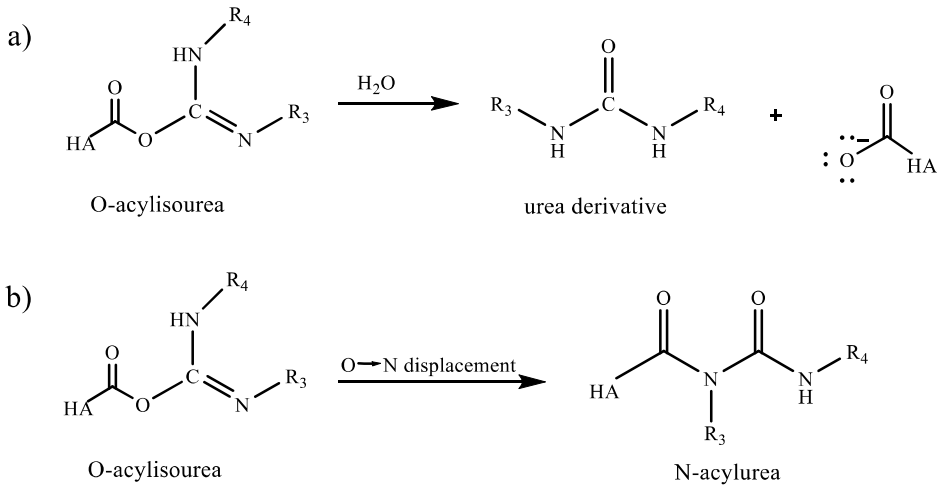

Figure 1.10. The reaction scheme of a) hydrolysis process of O-acylisourea and b) cyclic electronic displacement from oxygen to nitrogen

Bulpitt and Aeschlimann [38] used NHS and HOBt to avoid the formation of a stable N-acylurea product, and suggested that O-acylisourea was not active enough to react with primary amines. Instead, by using NHS and HOBt, they obtained an active ester intermediate, which was more stable against hydrolysis than O-acylisourea and was active towards primary amines. By performing the carbodiimide chemistry with NHS and HOBt, formation of stable N-acylurea was prevented (Figure 1.11).

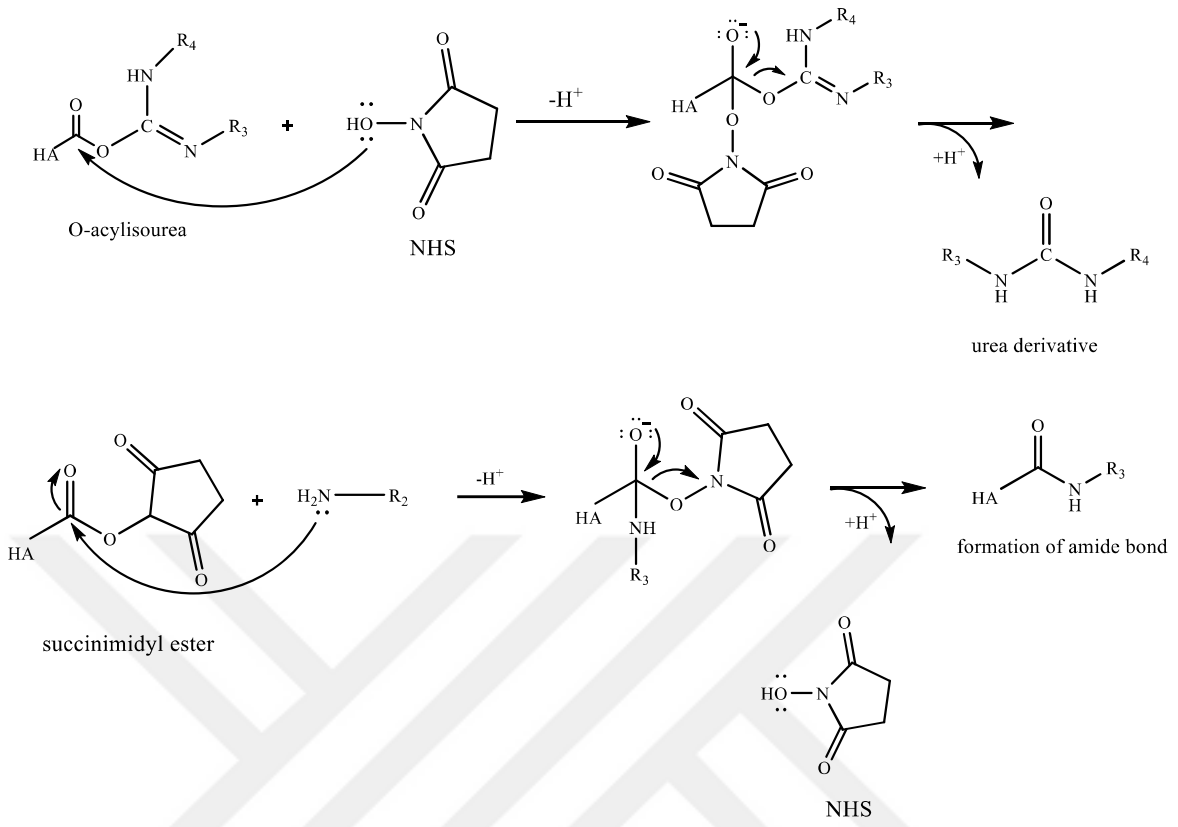

Figure 1.11. The reaction scheme of amide bond formation via producing hydrolysis stable- and active towards primary amine-succinimidyl ester.

1.3. Protein Encapsulation with Coacervation

Encapsulation is the process of covering or enclosing one material inside another one for a variety of applications. This method is a method utilized in a wide range of fields such as drug delivery, food industry, cosmetics and nanotechnology [40]. The method of encapsulation plays a crucial role, especially in the field of medicine because of the efficient delivery of bioactive substances and ability to protect sensitive bio-based materials. These bio-based substances like proteins are prone to degradation by pH, temperature and organic solvents. Effective encapsulation methods can be used to protect proteins from environmental stress and enhance their stability [41].

According to the literature, the encapsulation techniques are divided into three groups: chemical, physico-chemical and physico-mechanical. The method of encapsulation by using coacervation falls into the category of physico-chemical techniques. Complex coacervation,

which is a method based mainly on electrostatic interactions between oppositely charged groups, is considered as a very effective concept for protein entrapping [42,43].

Along with electrostatic interactions, hydrogen bonding and van der Waals interactions may also play an effective role in coacervation. During protein-encapsulation via complex coacervation, the electrostatic interactions between the polymers and proteins lead to the formation of spherical coacervate droplets, in which protein is entrapped. The efficiency and the stability of these droplets depend on the characteristics of the proteins and the polymers such as isoelectric point of proteins, dissociation constant of the protein/polymer complex, and the structure of proteins and polymers [44].

In the study of Zhao and and Zacharia [45], the aim was to encapsulate BSA within a complex coacervation system composed of a mixture of poly(acrylic acid) PAA and poly(allylamine) PAH to protect BSA from harsh conditions like pH, high temperature and urea treatment. They investigated the effect of various factors such as the mixing order, molar ratio of polyelectrolytes, concentration of polyelectrolytes and proteins using methods like dynamic light scattering (DLS), zeta potential, and circular dichroism (CD) spectroscopy, where the last technique was used to detect the denaturation of BSA.

2. AIM OF THE STUDY

The aim of this study is to synthesize hyaluronic acid-based polyampholytes (PA) with different grafting ratios by utilizing 1,4-Diaminobutane dihydrochloride (DN), adipic dihydrazide (ADH), and ethylenediamine dihydrochloride (EDA) via carbodiimide chemistry. These synthesized polyampholytes are characterized with ^{1}H-Nuclear Magnetic Resonance (^{1}H-NMR) and Fourier-Transform Infrared (FTIR) spectroscopy to analyze their chemical structure. Additionally, zeta potential experiments are performed to determine the isoelectric points (pI) of the polyampholytes. The main goal is to use these polyampholytes for the encapsulation of enzymes with different isoelectric points, such as alpha-chymotrypsin (αCT) (pI = 8.76), carbonic anhydrase (CA) (pI = 5.9), and lysozyme (LYS) (pI = 11). To optimize the encapsulation process, turbidimetric titration experiments are conducted to investigate the complexation behavior under varying pHs and sodium chloride (NaCl) concentrations.

3. EXPERIMENTAL SECTION

3.1. Materials

The sodium hyaluronate (HA), viscosity-average molecular weight (M_v) of which is given as 229 kDa by the manufacturer, was purchased from Lifecore Biomedical (Chaska, MN, USA).

N-(3-Dimethylaminopropyl)-N′-ethyl carbodiimide hydrochloride (EDC, ≥98.0%, Cat# = 03450-5G) was used as a water-soluble crosslinker agent to synthesize the amide bond between a negatively charged carboxylate (COO^-) group and a positively charged amine (NH_3^+) group. N-Hydroxysuccinimide (NHS, 98%, Cat# = 130672-5G) and 1-hydroxybenzotriazole (HOBt, ≥97.0%, Cat# = 54802-10G-F) were used to obtain an active-ester during the carbodiimide reaction. EDC, NHS and HOBt materials were all obtained from Sigma-Aldrich-Merck (St. Louis, MO, USA).

1,4-Diaminobutane dihydrochloride (DN, ≥99.0%, Cat# = 32810-25G), adipic dihydrazide (ADH, ≥97.0%, Cat# = 8.41689.0050) and ethylenediamine dihydrochloride (EDA, 98+%, Cat# = 187651000), which were used for amination of hyaluronic acid (HA) to obtain different grafting ratios of polyampholytes, were purchased from Sigma-Aldrich (St. Louis, MO, USA), Sigma-Aldrich-Merck (Darmstadt, Germany) and Thermo Scientific™ (Massachusetts, USA), respectively. Dimethyl sulfoxide (DMSO, synthesis grade, ≥ 99%), which was used to increase the solubility of HOBt and to avoid the hydrolysis of EDC, was purchased from Merck (Darmstadt, Germany).

Sodium chloride (NaCl, analysis grade) and ethanol (EtOH) absolute (analysis grade, ≥99.9%), which were used for precipitation during the purification step, were obtained from Sigma-Aldrich-Merck (Darmstadt, Germany) and ISOLAB (Eschau, Germany), respectively.

1-Butanol (analysis grade, ≥99.5%) and acetic acid (AcOH, 100%), which were used as solvents for thin layer chromatography (TLC) to detect amine groups, were purchased from Merck (Darmstadt, Germany) and VWR (Radnor, Pennsylvania, USA) respectively. For TLC analysis, TLC silica gel 60 F_{254} were obtained from Merck (Darmstadt, Germany). Ninhydrin (analysis grade, Cat# = 1.06762.0010, which was used for detection of amines, was purchased from Sigma-Aldrich-Merck (Darmstadt, Germany) to prepare its solution within EtOH containing 3% AcOH.

Poly(sodium 4-styrenesulfonate) (PSS, average M_w~70,000, powder, viscosity 15-55 cP, 20% (25 °C, Brookfield), Lot # = BCBF1832V, Cat # = 243051-5G) and bovine serum albumin (BSA, lyophilized powder, M_w ~ 66 kDa, purified by heat shock fractionation, protease free, fatty acid free, essentially globulin free, ≥98%, Lot # = 049K1635, Cat # = A7030-10G), which were used for preliminary turbidity experiments, were both purchased from Sigma-Aldrich (St. Louis, MO, USA).

α-Chymotrypsin from bovine pancreas (Type II, lyophilized powder, ≥ 40 units/mg protein, Cat # = C4129-1G), carbonic anhydrase from bovine erythrocytes (lyophilized powder, ≥ .95%(SDS-PAGE), specific activity ≥3,500 W-A units/mg protein, Cat # = C2624-500MG) and lysozyme from chicken egg white (lyophilized powder, protein ≥90%, ≥ 40,000 units/mg protein, Cat # = SAE0152-1G) were purchased from Sigma-Aldrich-Merck (St. Louis, MO, USA).

The semi-permeable membranes, Snakeskin Tubes of 3500 g/mol (3.500 MWCO) (product code: 68035) were purchased from Thermo Scientific™ (Massachusetts, USA). Research-grade buffer solutions (pH: 2.00, 4.00, 7.00, and 10.00) used for calibration of meters and NaOH & HCl solutions (0.1 N and 1 N) used for pH adjustments were purchased from ISOLAB Chemicals (Wertheim, Germany).

0.45 μm cellulose acetate syringe filters, which were used to filter all solutions, were purchased from Labmarker (Istanbul, Turkey). Milli-Q water with a resistivity of 18.2 MΩ·cm were used for all experiments.

3.2. Methods

3.2.1. Synthesis of Polyampholytes

The HA-based random type of polyampholytes were synthesized using different compounds which contain primary diamine in their structures such 1,4-Diaminobutane dihydrochloride (DN), adipic dihydrazide (ADH) and ethylenediamine dihydrochloride (EDA) to obtain an amide bond with different degrees of grafting. In the part of synthesis of polyampholytes via carbodiimide chemistry, EDC was used as a zero-length crosslinker while NHS or HOBt as an ester. All reactions were done at room temperature. The applied methodology was adapted from the study of Bulpitt and Aeschlimann [38].

3.2.1.1. Synthesis of HA-DN Polyampholyte. Sodium hyaluronate (HA) (40 mg, 0.25 mmol as monomer concentration, 229 kDa) was dissolved in Milli-Q water at 3 mg/mL concentration. 1,4-diaminobutane dihydrochloride (7.5 mmol, 161.07 g/mol) (pKa = 10.8) [46] was added into HA solution in solid form. The pH of the reaction was adjusted to 7.5 with 0.1 N HCl and NaOH by using Milwaukee MW150 Max pH meter equipped with a Milwaukee MA917 glass probe electrode (Milwaukee, Szeged, Hungary). EDC (1 mmol, 191.7 g/mol) and NHS (1 mmol, 115.09 g/mol) were each dissolved in 1 mL Milli-Q water and added into the mixture composed of HA and DN. After the dropwise addition, the pH of the final mixture was adjusted to pH 7.5 and kept under control by adding 1 N NaOH or 0.1 N HCl. The reaction was allowed to continue overnight.

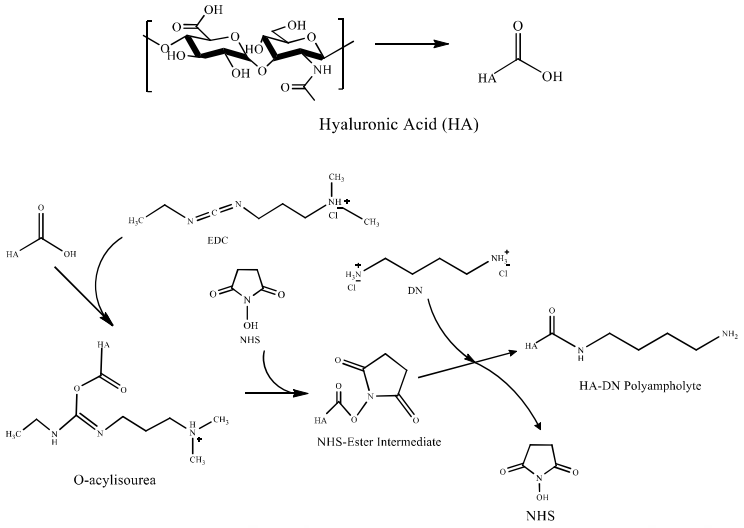

Figure 3.1. The general reaction scheme of HA-DN polyampholyte.

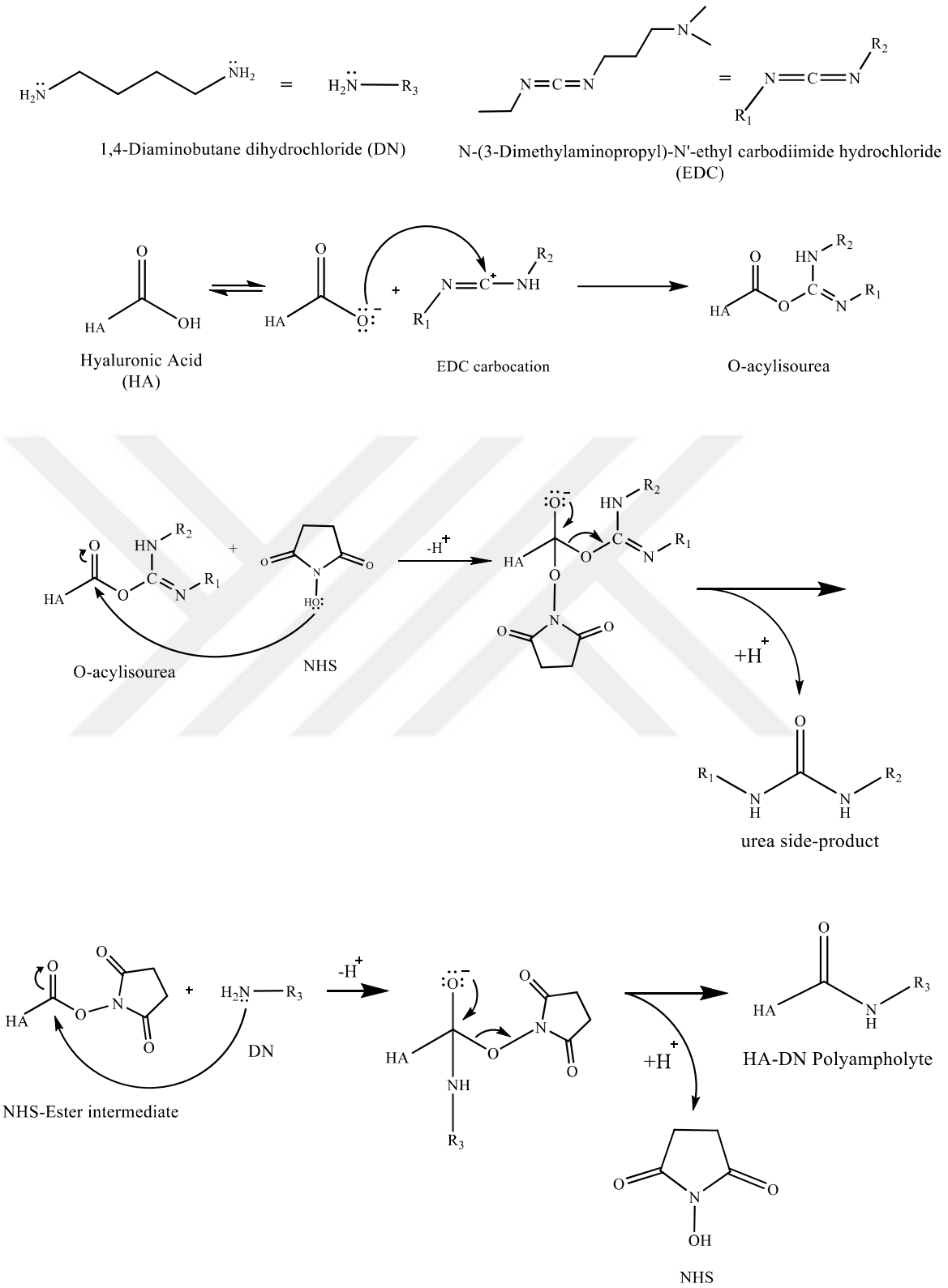

Figure 3.2. The reaction mechanism of HA-DN polyampholyte.

3.2.1.2. Synthesis of HA-ADH Polyampholyte. Sodium hyaluronate (HA) (40 mg, 0.25 mmol as monomer concentration, 229 kDa) was dissolved in Milli-Q water at 3 mg/mL concentration. Adipic dihydrazide (ADH) (7.5 mmol, 174.2 g/mol) (pKa = 2.5) [47] was added into HA solution in solid form. The pH of the reaction was adjusted to 6.8 with 0.1 N HCl and NaOH by using Milwaukee MW150 Max pH meter equipped with a MA917 glass probe electrode. EDC (1 mmol, 191.7 g/mol) and HOBt (1 mmol, 135.12 g/mol) were dissolved in the mixture composed of DMSO and H_2O with 1:1 ratio (by volume) added into the mixture of HA and ADH. After the dropwise addition, the pH of the final mixture was adjusted to pH 6.8 and kept under control by adding 1 N NaOH or 0.1 N HCl. The reaction was allowed to continue overnight.

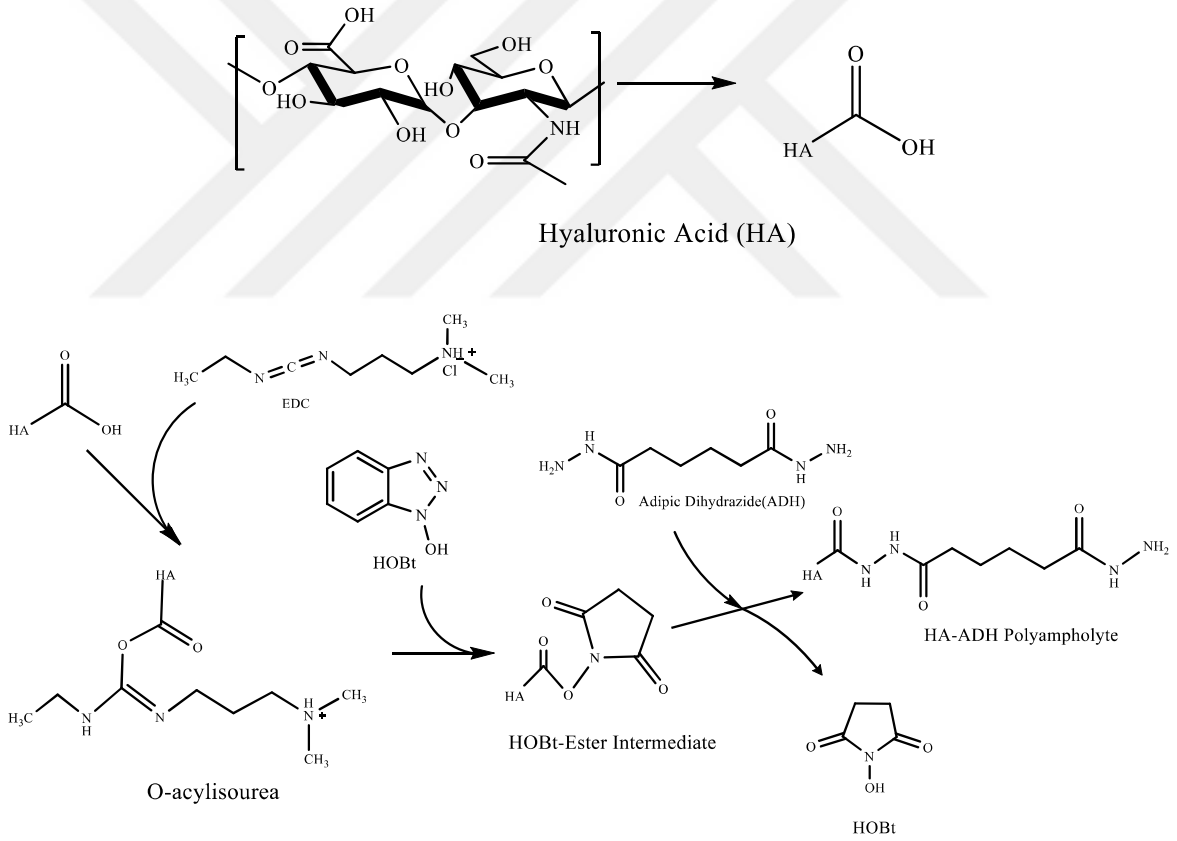

Figure 3.3. The general reaction scheme of HA-ADH polyampholyte.

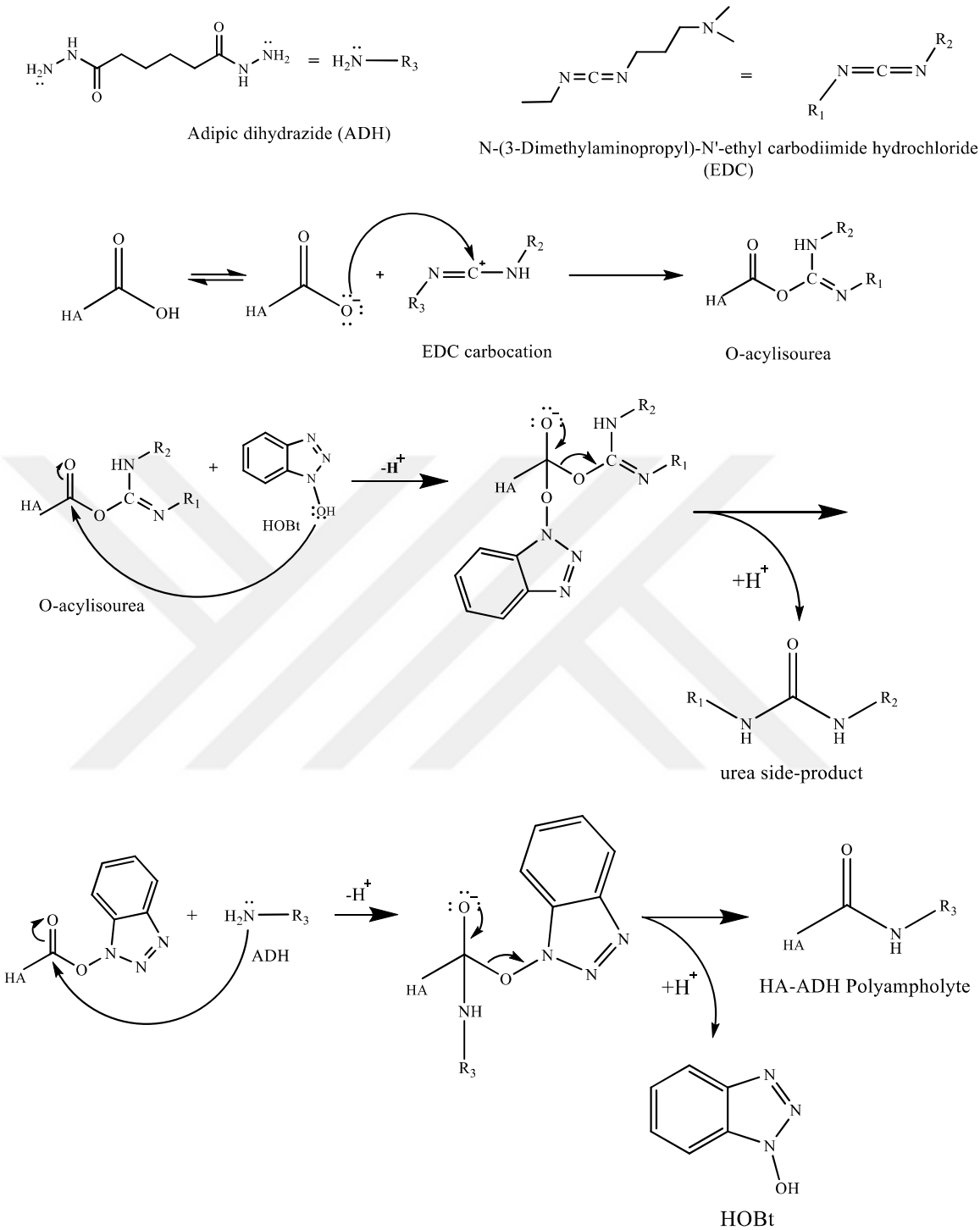

Figure 3.4. The reaction mechanism of HA-ADH polyampholyte.

3.2.1.3. Synthesis of HA-EDA Polyampholyte. Sodium hyaluronate (HA) (40 mg, 0.25 mmol as monomer concentration, 229 kDa) was dissolved in Milli-Q water at 3 mg/mL concentration. Ethylenediamine dihydrochloride (EDA) (7.5 mmol, 133.02 g/mol) (pKa_1 = 10.0 and pKa_2 = 7.1) [48] was added into HA solution in solid form. The pH of the reaction was adjusted to 6.8 with 0.1 N HCl and NaOH by using Milwaukee MW150 Max pH meter equipped with a MA917 glass probe electrode. EDC (4 mmol, 191.7 g/mol) and HOBt (4 mmol, 135.12 g/mol) were dissolved in the mixture composed of DMSO and H_2O with 1:1 ratio (by volume) and added into the mixture of HA and EDA. After the dropwise addition, the pH of the final mixture was adjusted to pH 6.8 and kept under control by adding 1 N NaOH or 0.1 N HCl. The reaction was allowed to continue overnight.

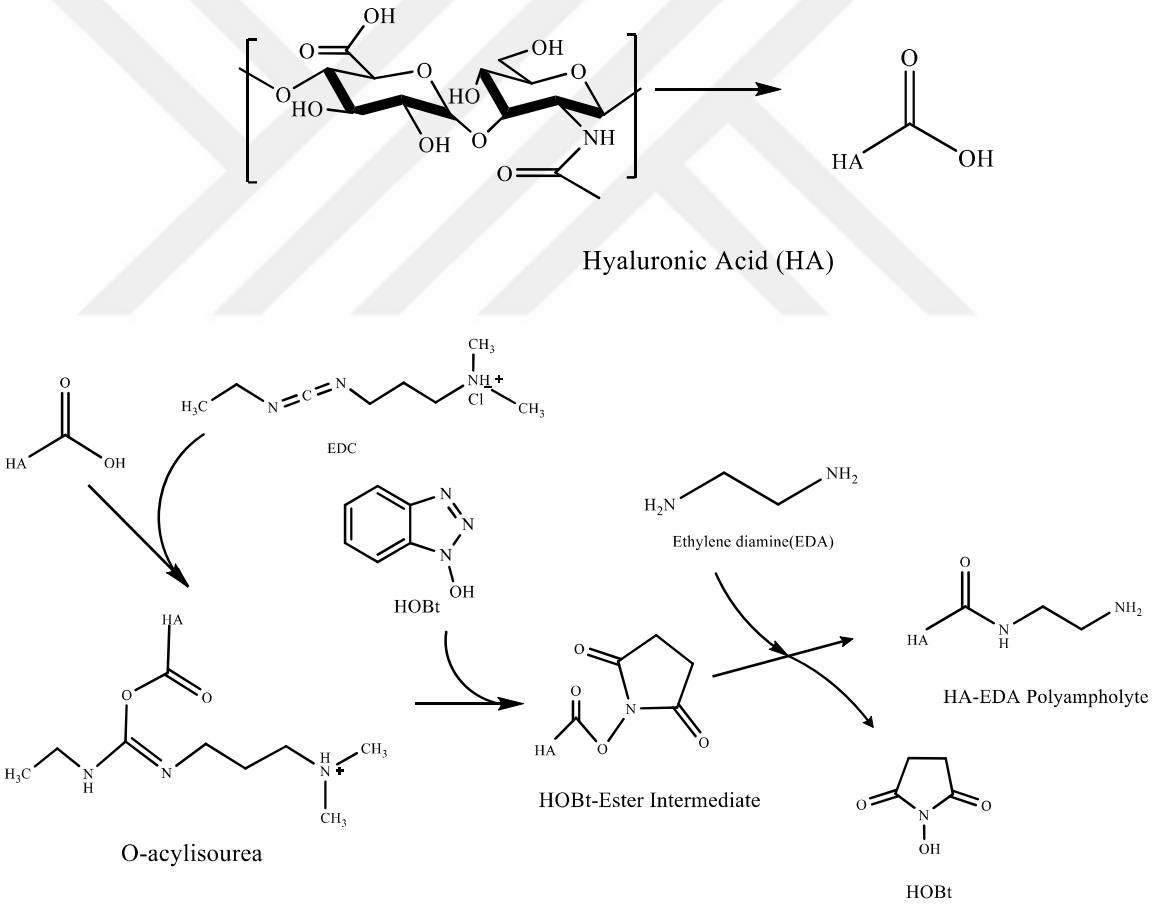

Figure 3.5. The general reaction scheme of HA-EDA polyampholyte.

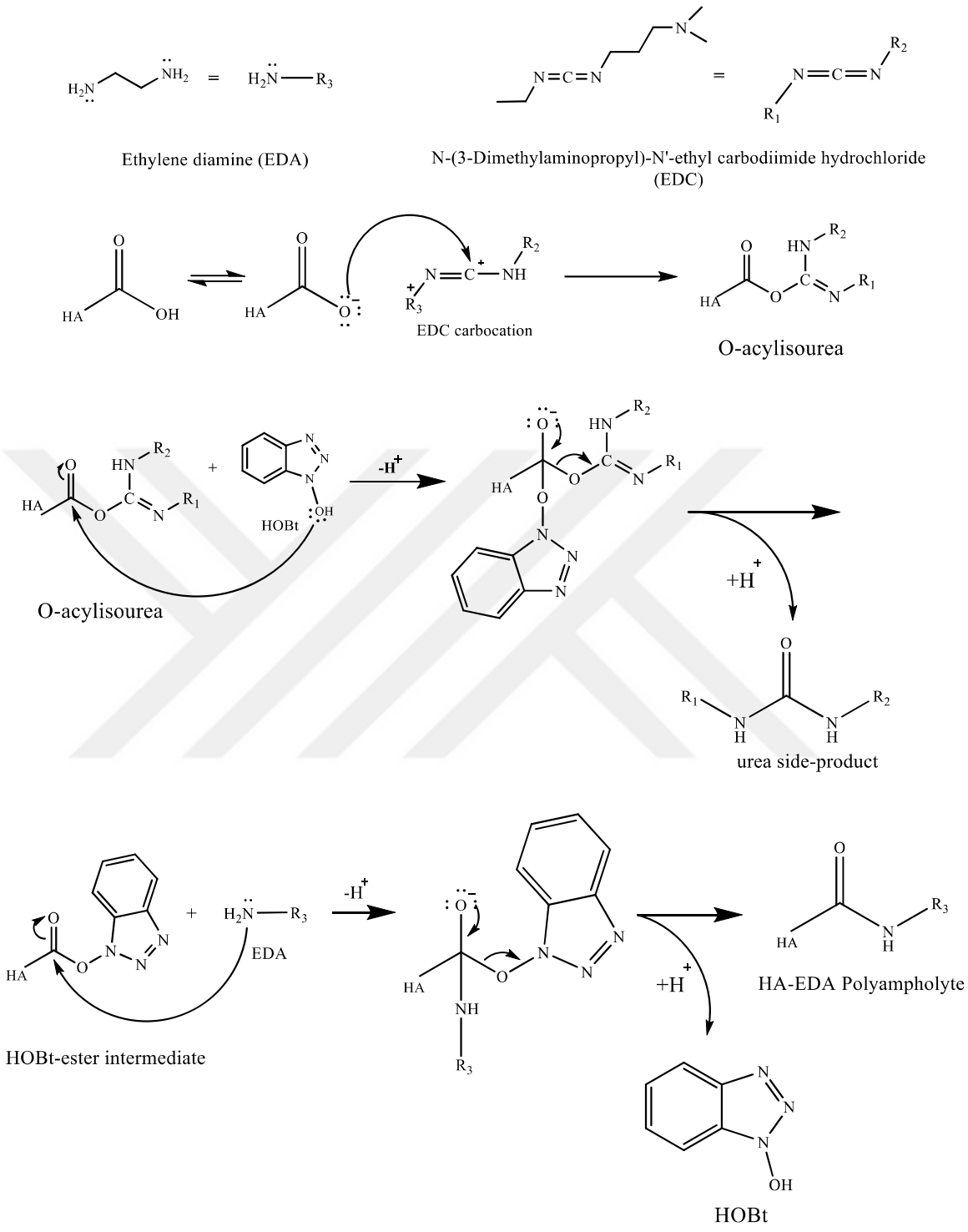

Figure 3.6. The reaction mechanism of HA-EDA polyampholyte.

3.2.2. Purification of Polyampholytes

The purification procedure, which includes 8 stages, was applied for all three types of synthesized polyampholytes.

- Step 1: Thin Layer Chromatography (TLC)
- Step 2: 1st Dialysis
- Step 3: Thin Layer Chromatography (TLC)
- Step 4: Precipitation
- Step 5: Vacuum Drying
- Step 6: 2nd Dialysis
- Step 7: Thin Layer Chromatography (TLC)
- Step 8: Lyophilization

Thin layer chromatography (TLC) was fundamentally used to detect the added excess amine into solution at every step of purification. For the mobile phase 1-Butanol: AcOH: H_2O mixture was used with 12:3:5 ratio (by volume) to obtain a 2 mL solution. After running the TLC, the TLC plate was dried with heat gun. The ninhydrin solution (2% w/v), which was prepared previously in EtOH with 3% AcOH by volume, was applied on the TLC plate to make the excess amine impurities visible with a color of Ruhemann purple (Figure 3.7) after drying with heat gun.

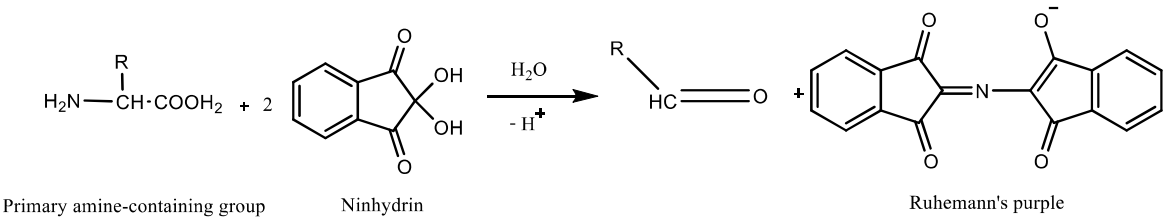

Figure 3.7. The reaction of scheme of ninhydrin treatment.

The first dialysis method was applied after 24 hours of reaction using semi-permeable membranes (3500 MWCO) against Milli-Q water for two days by changing the water three times a day to get rid of the small molecules such as excess amines, EDC and NHS or HOBt

depending on the synthesized polyampholytes and side products. After two days, just before the precipitation method, TLC method was re-applied to check for the impurities.

The method of precipitation was applied with adding 5% w/v NaCl. Then, cold EtOH was added at three times the volume of solution. The solution was kept in the fridge until complete precipitation. The precipitates were collected with using Z 206 A compact centrifuge instrument (Hermle, Germany) at 5000 rpm for 10 min. Then, vacuum drying process was applied using RV3 vacuum pump (Edwards, Sweden) until it dried. The mixture of ice and table salt was used as a cooling agent.

The solid obtained after the drying process was dissolved at 5 mg/mL concentration in Milli-Q water. The 2nd dialysis method was applied for 24 hours by changing the water three times a day. After a day of dialysis, the TLC method was applied for the last time, just before the lyophilization method. Finally, the purified solid form of polyampholytes was recovered by FreeZone 2.5 liter freeze-dry system (Labconco, Kansas City, MO).

3.2.3. ^{1}H-Nuclear Magnetic Resonance (^{1}H-NMR) Spectroscopy Measurements

^{1}H-NMR spectra of the purified polyampholytes in D_2O as a solvent at 5 mg/mL concentration were recorded by using a Varian Mercury-VX 400 MHz BB (Varian Associates, Palo Alto, CA) at the Advanced Technologies Research and Development Center at Bogazici University and Ultrashield 400 MHz (Bruker, Germany) at the Lifesci at Bogazici University.

3.2.4. Fourier-Transform Infrared Spectroscopy (FTIR) Measurements

The FTIR spectroscopies were recorded with using Nicolet 380 FT-IR spectrometer (Thermo Scientific™, Waltham, MA, USA).

3.2.5. Zeta Potential Measurements

The zeta potential measurements for unmodified HA and all synthesized polyampholytes, i.e. HA-DN, HA-ADH and HA-EDA, were carried out using a ZetaSizer NanoZS (Malvern, UK) instrument at 25 °C. All polymers with 3 mg/mL concentrations were prepared in 100 mM NaCl and filtered just before the experiments using 0.45 μm cellulose acetate syringe filters. The pH of the stock solution was adjusted from 2.0 to 8.0 with using 0.1 N NaOH. All measurements were run at least three times. In each measurement, 100 μL sample were loaded into the capillary cell filled with 100 mM NaCl via the method of diffusion barrier [49] The Malvern software utilized the Smoluchowski equation to transform the electrophoretic mobility of the polymers into a ζ-potential [50,51].

The technique of diffusion barrier was used for loading the sample into Zetasizer folded capillary disposable cell (DTS1070). Small sample volumes (20-100 μl) and buffers with high ionic strength are suited for this technique. A small volume of the sample is carefully injected into the bottom part of the capillary tube, which is prefilled with the solvent only used for the preparation of sample. The focus is to keep the sample away from the electrodes in order to directly block the contact and avoid the electrode blackening which could adversely affect the results [52].

3.2.6. Turbidimetric pH Titrations

The method of turbidimetric pH titrations were done to investigate the phase diagram of polyampholytes with different types of polymers or proteins such as PSS, BSA, α-CT, CA and LYS at different salt concentrations. Turbidimetric pH titration experiments were done with a 2 cm path length fiber optic probe colorimeter (Brinkmann PC 950) with a filter of 420 nm and Thermo Scientific Orion 3 Star Benchtop pH meter combined with Mettler Toledo pH electrode InLab Flex-Micro (Type No: 51343164). 0.1 N HCl or 0.1 N NaOH was used as a titrant solution depending on the pH direction of the titration. The percent transmittance (% T) of the titrated solution is measured steadily and then converted to turbidity which is calculated as 100 - % T = % Turbidity. The interaction strength between the macromolecules could be qualitatively determined by using turbidimetric titrations.

4. RESULT AND DISCUSSION

The fundamental aim is to synthesize hyaluronic acid-derived polyampholytes using different amines such as 1,4-diaminobutane dihydrochloride (DN), adipic dihydrazide (ADH) and ethylenediamine dihydrochloride (EDA). The polyampholytes including HA-DN, HA-ADH and HA-EDA were characterized with ^{1}H-NMR spectroscopy and FTIR.

4.1. ^{1}H-Nuclear Magnetic Resonance (^{1}H-NMR) Spectroscopy

^{1}H-NMR spectroscopy allows one to analyze the modified structure of hyaluronic acid with respect to the newly attached functional groups. The degree of substitution of hyaluronic acid with amines are also determined via integration of specific signals from hydrogen atoms in ^{1}H-NMR. In addition, this technique enables detection of impurities and side products in the sample.

The methyl (-CH_3) resonance (^{1}H-NMR (D_2O) δ = ~2.0 (bs, 3H, HA-NHCO.C*H*$_3$)) peak of acetamido moiety of the N-acetyl-D-glucosamine was used as an internal standard for characterization of the polyampholytes to calculate their degree of substitution (D.S.). The broad signal between δ = 3.00 ppm and δ = 4.00 ppm was assigned as signals of hydrogens in sugar rings. The broad peak which is around δ = 4.5 ppm corresponds to two anomeric protons which are located on the carbons connected to the two oxygen atoms (Figure 4.1).

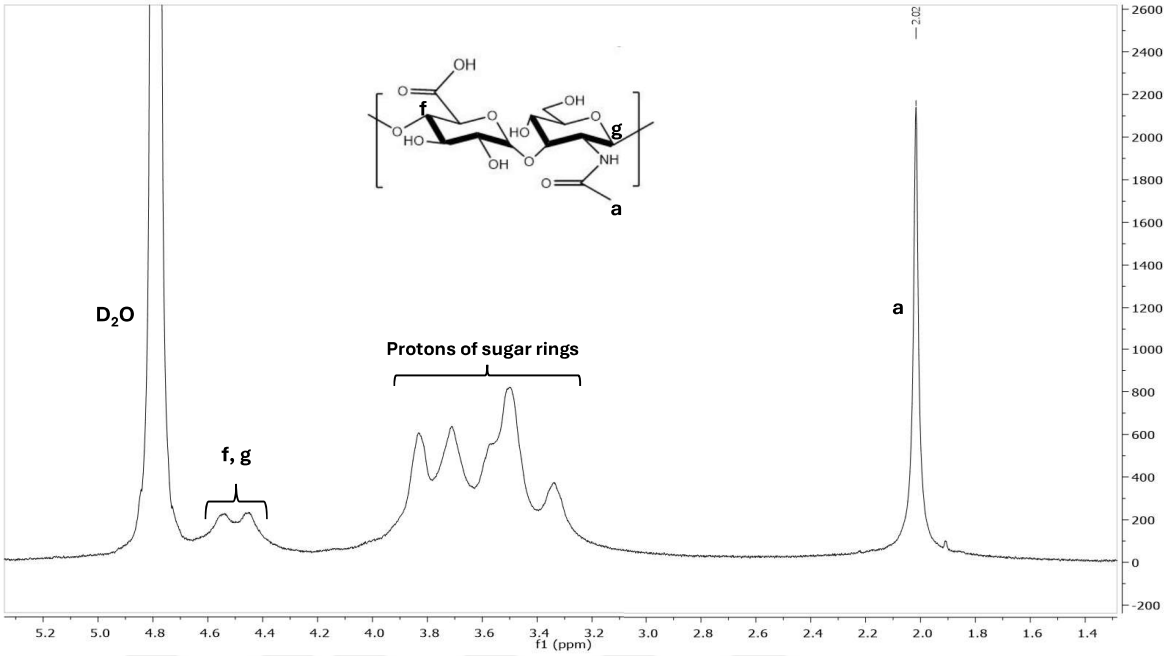

Figure 4.1. ^{1}H-NMR spectrum of unmodified HA.

4.1.1. ^{1}H-Nuclear Magnetic Resonance (^{1}H-NMR) Spectroscopy of HA-DN

Hyaluronic acid was modified with 1,4-Diaminobutane dihydrochloride (DN) via carbodiimide chemistry using EDC and NHS, as mentioned in the synthesis part of the methodology. The modification of HA to HA-DN polyampholyte was characterized by ^{1}H-NMR spectroscopy. As it can be seen from Figure 4.2, the signal labelled with "a" represents the -CH_3 protons (δ = 2.03, bs, 3H, HA-NHCO.CH_3) which belongs to unmodified hyaluronic acid structure, and is used as an internal reference. Preparation of HA-DN polyampholyte was confirmed by the appearance of protons of the attached group of diamines; i.e.δ 3.15-3.05 (m, 4H, CO. NHCH_2, CH_2NH_2), δ 1.69–1.56 (dm, 4H, CH_2CH_2).

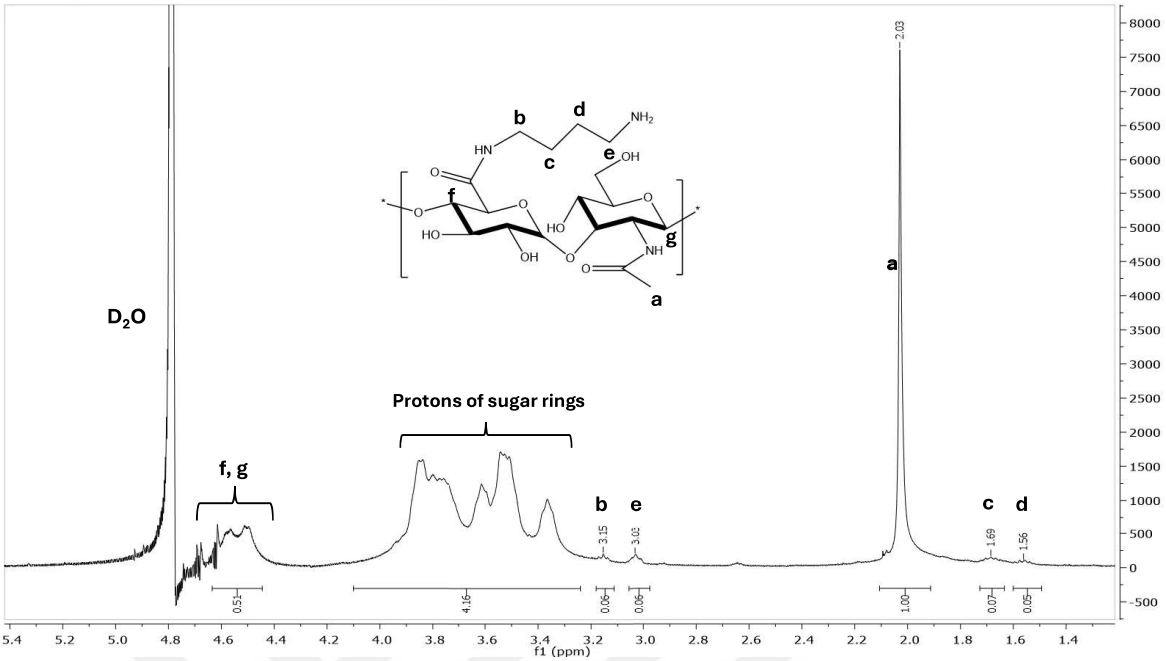

Figure 4.2. ^{1}H-NMR spectrum of HA-DN polyampholyte.

The apparent degree of substitution for HA-DN was about 10 ± 2 %, which was calculated by using the internal standard and the attached group of protons. Since the aim of our investigation was to obtain polyampholytes with different grafting ratios, solvent type, mole ratios of DN: EDC: NHS, mixing order of reagents and temperature were varied at different trials (Table 4.1). However, the degree of substitution stayed constant at around 10 % although the mentioned changes were implemented.

Table 4.1. The varied parameters to obtain a higher degree of substitution for HA-DN.

Parameters		Degree of substitution (D.S.)
Solvent type	Milli-Q water	10 ± 2 %
	0.1 M MOPS	
	THF: H_2O with different volume ratios	
Mole ratio of reagents (DN: EDC: NHS)	30: 4: 4	
	30: 8: 8	
	50: 4: 4	
Mixing order	HA-DN-EDC-NHS	
	HA-EDC-NHS-DN	
Temperature	Room temperature	
	0 °C	

The reason behind the result of a low degree of substitution was related to the pK_a value of the diamine, a.k.a. DN. The pK_a of DN is equal to 10.8 [46] while the pH at which the reaction is performed is 7.5. As a consequence, during the reaction, the functional group of the diamine is mostly protonated, i.e. $-NH_3^+$. However, the amine groups should be deprotonated ($-NH_2$) to attack the NHS-ester intermediate to obtain the polyampholyte (Figure 3.2). Thus, the majority of the amine groups are in the protonated state since the pH value is far from the pK_a value of DN, which is the main reason of having a low degree of substitution. In other words, there are only a few deprotonated amines in the medium that can react with the active-ester intermediate.

4.1.2. ^{1}H-Nuclear Magnetic Resonance (^{1}H-NMR) Spectroscopy for HA-ADH

Hyaluronic acid was modified with adipic dihydrazide (ADH) via carbodiimide chemistry using EDC and HOBt, as mentioned in the synthesis part of the methodology. The modification of HA to HA-ADH polyampholyte was characterized by using ^{1}H-NMR spectroscopy. As it can be seen from Figure 4.3, the signal labelled with “a” represents the $-CH_3$ protons (δ = 2.01, bs, 3H, HA-NHCO.C*H*$_3$) which belongs to unmodified hyaluronic

acid structure, and is used as an internal reference. Preparation of HA-ADH polyampholyte was confirmed by the appearance of protons of the attached group of diamines; i.e. δ 2.41 (m, 2H, NHNHCO.CH_2), 2.27 (m, 2H, CH_2NHNH_2), 1.65 (m, 4H, CH_2CH_2).

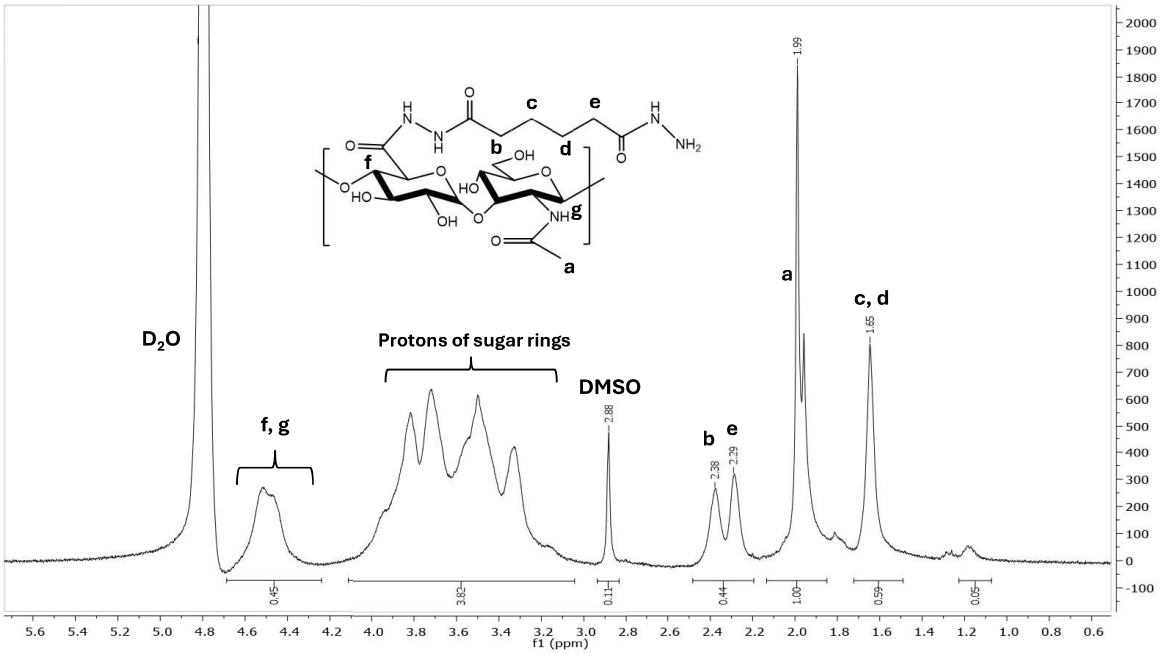

Figure 4.3. ^{1}H-NMR spectrum of HA-ADH polyampholyte.

When ADH was replaced with DN in the carbodiimide reactions, HA-ADH polyampholytes with different degree of substitutions, ranging from ~20 % to ~40 %, could be obtained by changing the molar ratios of ADH, EDC and HOBt with respect to HA. However, the most reproducible degree of substitution was 40 ± 2 % which was obtained with the mol ratios of 1:30:4:4 for HA: ADH: EDC: HOBt, respectively.

In order to decrease the degree of substitution with an aim of obtaining PA's with different amounts of amine groups, we then worked on reducing the amount of reagents used. The mole ratios of 1:0.5:1:1 and 1:0.5:4:4 for HA: ADH: EDC: HOBt were tried on a small scale (initial mass of HA=15 mg), to obtain 20% and 30% degree of substitutions, respectively. Reproducible results were obtained without any complication due to gelation. Upon setting up reactions on a large scale (initial mass of HA=40 mg), the problem of gelation during the dissolution process in Milli-Q water after the 2nd dialysis arose. The

origin of this gelation was most likely unrelated to the ratios of EDC and HOBt since the ADH ratio was kept constant in both cases.

Schanté and coworkers used excess diamine to overcome this problem [53]. The reason behind this complication was crosslinking between diamines and HA. The form of amine should be used as a diamine to obtain an amide bond between carboxyl group and amine(-NH_2) terminated polymer chain.

The primary problem was the formation of a crosslink with diamines due to the reaction capability of the two functional end groups. If both of these end groups bind to different carboxyl groups of HA, a water-insoluble crosslinked polymer gel is obtained. In order to reduce the possibility of getting crosslinks, the number of moles of diamines that can react in the environment is increased to 30-folds (in moles) with respect to HA so that an amine will not form an amide bond from both of its sides. Therefore, excess diamine was used at the rest of the experiments to modify the HA to obtain a polyampholyte.

4.1.3. ^{1}H-Nuclear Magnetic Resonance (^{1}H-NMR) Spectroscopy for HA-EDA

Hyaluronic acid was modified with ethylene diamine (EDA) via carbodiimide chemistry using EDC and HOBt, as mentioned in the synthesis part of the methodology. The modification of HA to HA-EDA polyampholyte was characterized by using ^{1}H-NMR spectroscopy. As it can be seen from Figure 4.4, the signal labelled with “a” represents the -CH_3 protons (δ = 2.00, bs, 3H, HA-NHCO.C*H*$_3$) which belongs to unmodified hyaluronic acid structure and is used as an internal reference. Preparation of HA-EDA polyampholyte was confirmed by the appearance of the protons of the attached group of diamines; i.e. δ 3.16 (m, 2H, (-CO-NH-CH_2-*C*H_2-NH_2)).

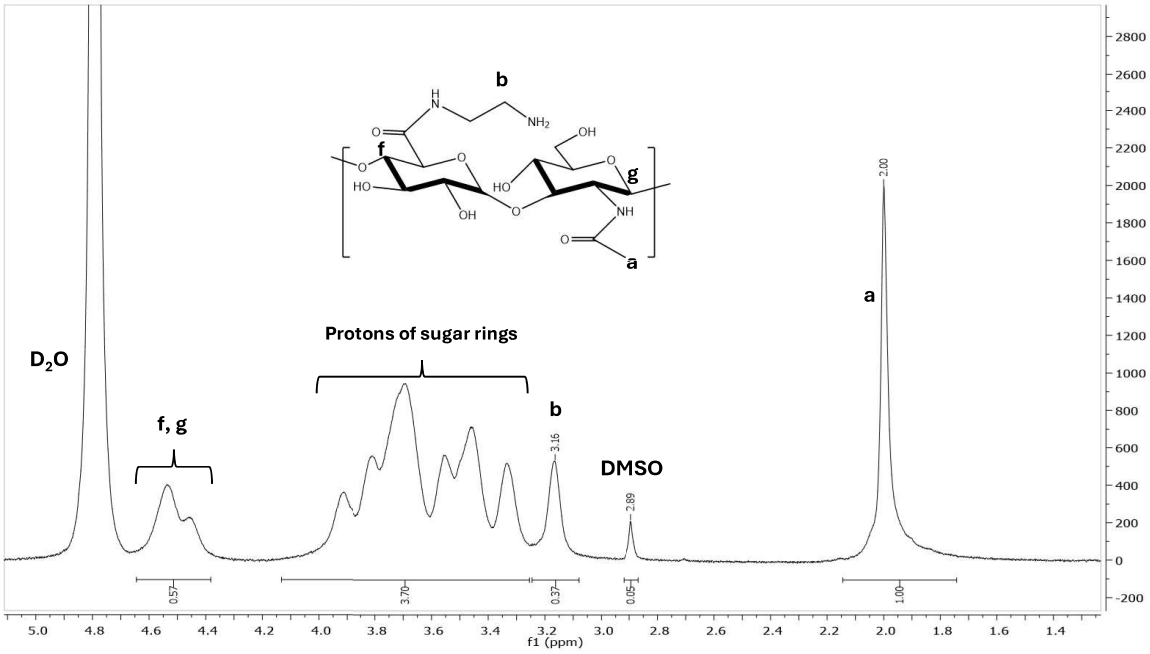

Figure 4.4. ^{1}H-NMR spectrum of HA-EDA polyampholyte.

The main aim of replacing ADH with EDA was to have a high degree of substitution without having a dihydrazide in the chemical structure. The pKa of EDA is lower than DN, so the expected degree of substitution will be higher than HA-DN polyampholyte. When the proportion between "a" and "b" labelled hydrogens was used to calculate degree of substitution, the degree of substitution was found 50 ± 3 %.

4.2. Fourier-Transform Infrared (FTIR) Spectroscopy

FTIR spectroscopy was used to detect the newly attached amine groups and the amide bond formed in the polyampholytes by comparing it with the spectra of unmodified HA. In addition, this technique was used as a detection method for impurities. The vibration of -OH and -NH bonds which were characteristic of HA was observed at 2900-3700 cm^{-1}, the vibration of C-H bonds at 2800-2900 cm^{-1}, the vibration of C=O carbonyl group at 1607 cm^{-1}, and the vibration of C-O-C ester bonds at 1037 cm^{-1} [54]. The signals in the range of 2355-2360 cm^{-1} belong to CO_2 (O=C=O) in the environment (Figure 4.5) [55].

The newly attached amine (-NH_2) groups via carbodiimide chemistry were hindered by the broad peak of -NH and -OH bonds which were present in the structure of unmodified HA. Thus, the modification of HA was followed by the reduction of sharpness and the left shift of the vibration of the C=O bond at 1607 cm^{-1} [56]. As the concentration of the pure carbonyl (-C=O) bonds diminishes by conversion into amide bonds, the sharpness of the peak is reduced.

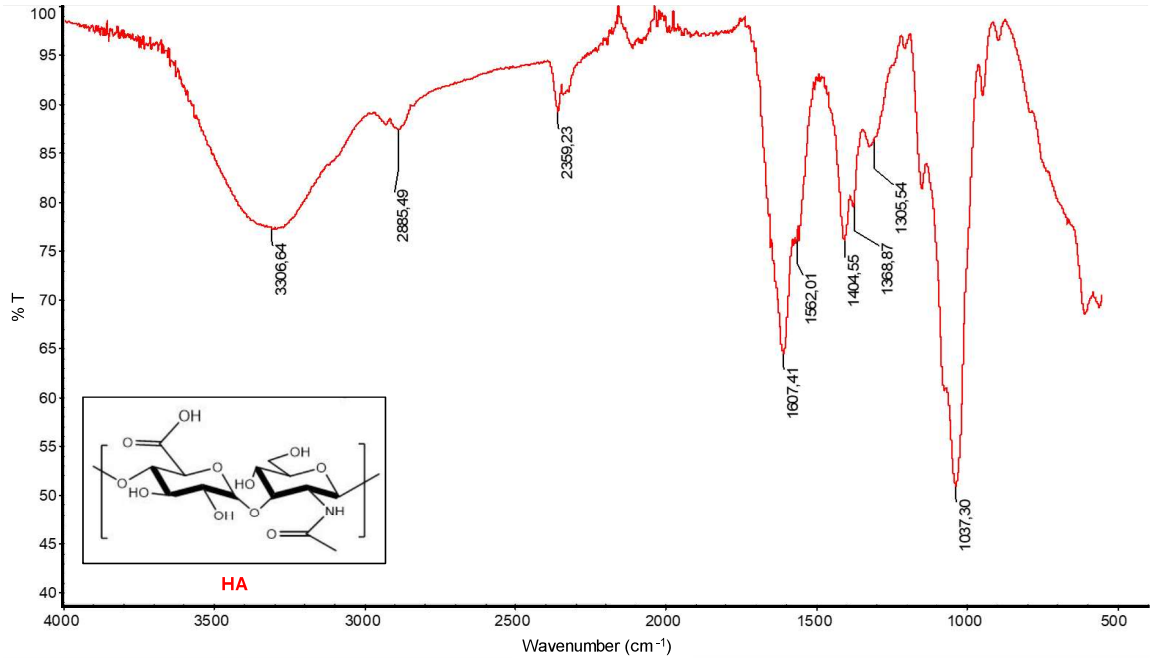

Figure 4.5. FTIR spectrum of unmodified HA.

4.2.1. Fourier-Transform Infrared (FTIR) Spectroscopy for HA-DN

The modification of HA as a polyampholyte can be traced by the left shift of the carbonyl(-C=O) at 1607 cm^{-1}. In the Figure 4.6, the red line belongs to HA-DN polyampholyte with ~10% degree of substitution and the blue one belongs to the native HA sample. As it can be observed form the related figure (Figure 4.4), when the carbonyl group transforms into amide bond, the peak shifts left from 1607 cm^{-1} to 1644 cm^{-1} and the steepness of this peak decreases. In addition to that, the signal about at 1550 and 1560 cm^{-1} called amide 2 peak represents the -C-N- stretching [57]. With the increasing of the -C-N- bond amount after modification, this peak became more visible.

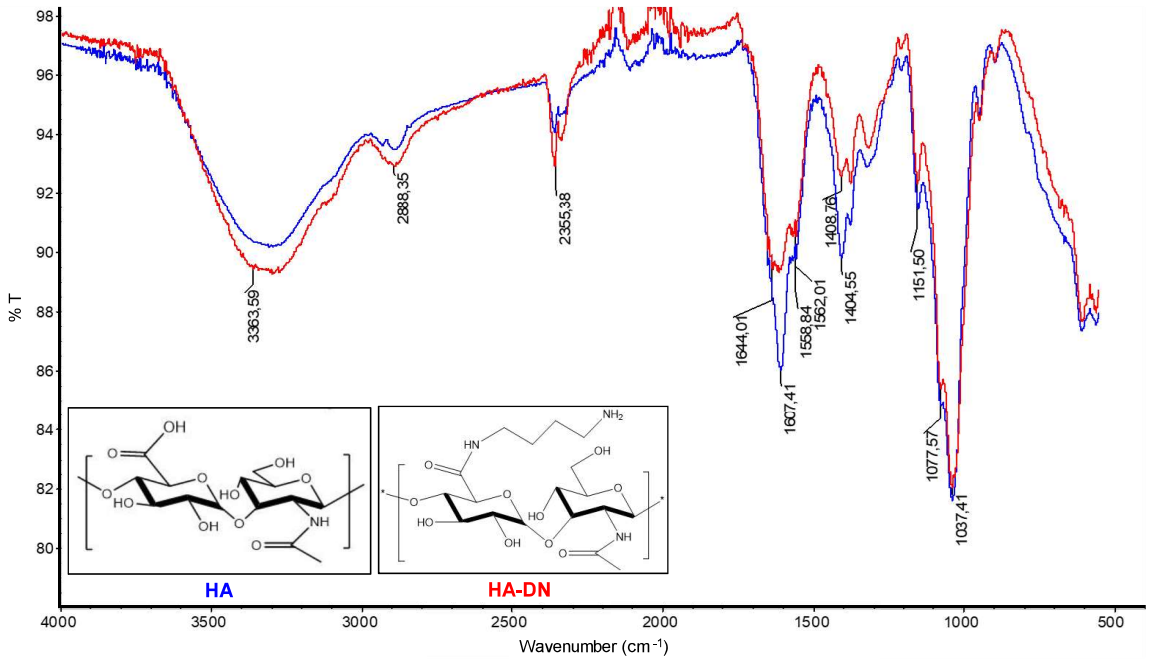

Figure 4.6. The comparative FTIR spectrum of HA-DN and unmodified HA.

4.2.2. Fourier-Transform Infrared (FTIR) Spectroscopy for HA-ADH

The modification of HA into a polyampholyte can be traced by the left shift of the carbonyl (-C=O) peak at 1607 cm^{-1}. In the Figure 4.7, the red line belongs to HA-ADH polyampholyte with 40 ± 2 % degree of substitution and the blue one belongs to the unmodified HA sample. As it can be seen from Figure 4.4, when the carbonyl group transforms into an amide bond, the peak shifts left from 1607 cm^{-1} to 1651 cm^{-1} and the steepness of this peak decreases. In addition to that, the signal about at 1550 and 1560 cm^{-1}, which is designated as the amide II peak, represents the -C-N- stretching [57]. With the increase of the amount of -C-N- bond after modification, this peak becomes more visible.

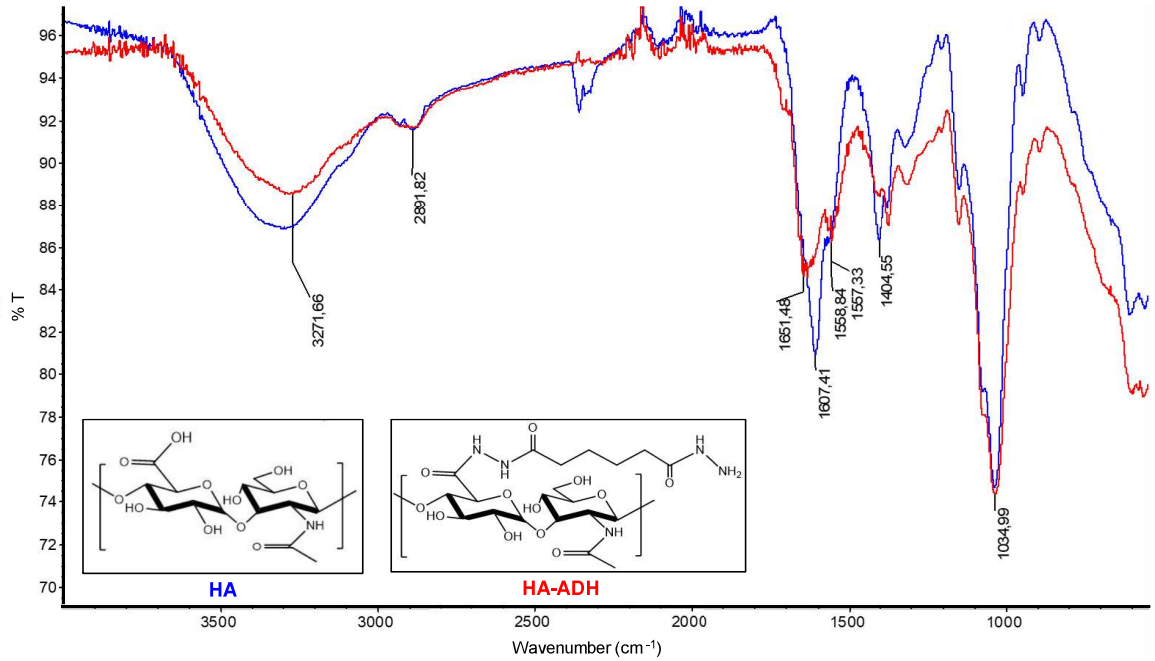

Figure 4.7. The comparative FTIR spectrum of HA-ADH and unmodified HA.

4.2.3. Fourier-Transform Infrared (FTIR) Spectroscopy of HA-EDA

The modification of HA into a polyampholyte can be traced by the left shift of the carbonyl (-C=O) peak at 1607 cm^{-1}. In Figure 4.8, the red line belongs to HA-EDA polyampholyte with 50 ± 3% degree of substitution and the blue one belongs to the unmodified HA sample. As it can be seen from Figure 4.4, when the carbonyl group transforms into an amide bond, the peak shifts left from 1607 cm^{-1} to 1650 cm^{-1} and the steepness of this peak decreases. In addition to that, the signal between 1550 and 1560 cm^{-1}, designated as amide II peak, represents the -C-N- stretching [57]. With the increase of the amount of -C-N- bond after modification, this peak becomes more visible.

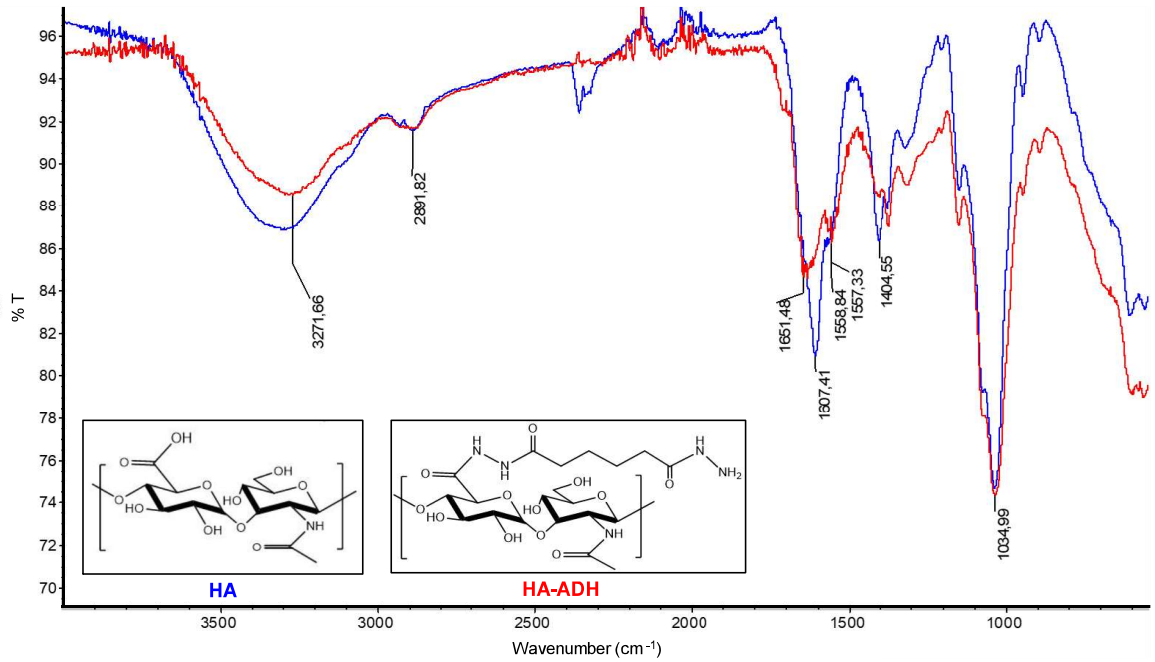

Figure 4.8. The comparative FTIR spectrum of HA-EDA and unmodified HA.

In conclusion, the leftward shift from 1607 cm^{-1} to 1644 cm^{-1} (HA-DN) and 1650 cm^{-1} (HA-ADH and HA-EDA) is positively correlated with the degree of substitution.

4.3. Zeta Potential

Hyaluronic acid (HA) is a natural biopolymer with carboxyl groups (-COOH) which dissociate to carboxylate anions ($-COO^-$) in solution. The pK_a value, generally around 3-4[58], represents the pH at which half of these carboxyl groups are dissociated, which provides an understanding of the ionization state of hyaluronic acid under several pH conditions. However, when HA is chemically modified with diamine via carbodiimide chemistry to have both positive and negative charge groups, it transforms into an ampholytic macromolecule. This modification results in appearance of an isoelectric point (pI), which is the pH at which the net charge of the polymer is equal to zero, when the positive and negative charges are in balance. Thus, zeta potential experiments were conducted to investigate the isoelectric point (pI) of polyampholytes derived from hyaluronic acid.

Table 4.2. Zeta potentials of polyampholytes and unmodified HA at different pHs.

Zeta Potential (mV)				
pH	**HA (unmodified)**	**HA-DN (D.S.: 10%)**	**HA-ADH (D.S.: 40%)**	**HA-EDA (D.S.: 50%)**
1.00 ± 0.05	-	0.801 ± 0.059	-	-
2.00 ± 0.05	-5.995 ± 2.213	-6.323 ± 1.123	3.423 ± 0.707	5.140 ± 0.078
3.00 ± 0.05	-12.433 ± 1.159	-9.157 ± 1.985	-5.190 ± 1.643	-0.585 ± 0.102
4.00 ± 0.05	-15.100 ± 1.217	-14.033 ± 1.721	-10.500 ± 0.356	-4.270 ± 0.237
5.00 ± 0.05	-16.967 ± 2.303	-13.800 ± 0.755	-12.133 ± 1.552	-4.673 ± 0.077
6.00 ± 0.05	-14.500 ± 2.166	-16.133 ± 1.002	-12.033 ± 0.776	-5.387 ± 0.097
7.00 ± 0.05	-14.700 ± 2.066	-16.333 ± 1.270	-11.833 ± 0.368	-5.270 ± 0.376
8.00 ± 0.05	-12.766 ± 1.041	-17.000 ± 1.375	-12.967 ± 0.047	-5.560 ± 0.651

The zeta potential measurements were done in 100 mM NaCl at 3mg/mL polymer concentration with using diffusion barrier method, as it is mentioned in methodology part. Zeta potential measurements, which are given in Table 4.2., were repeated at least three times for each pH of each polyampholyte. In zeta potential measurements conducted at different pH's, no significant difference was observed between unmodified HA and HA-DN (D.S.: 10%) polyampholyte. However, a noticeable difference was observed with HA-ADH (D.S.: 40%) and HA-EDA (D.S.: 50%) polyampholytes when compared to the unmodified HA zeta potential data.

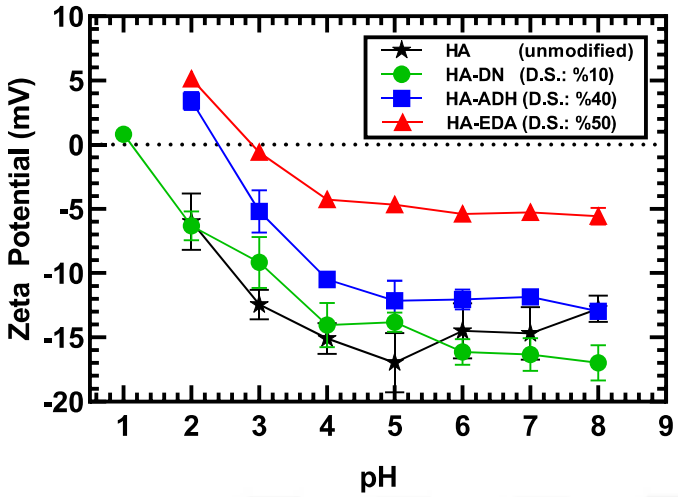

Figure 4.9. Zeta potential versus pH graph for HA-derived polyampholytes and unmodified HA.

As seen in Figure 4.9, the point where the plot crosses with the x-axis is determined as the isoelectric point at which the net charge of the polyampholyte is zero.

Table 4.3. Isoelectric points of polyampholytes.

	Isoelectric Point (pI)
HA-DN (D.S.: 10%)	1.110 ± 0.015
HA-ADH (D.S.: 40%)	2.401 ± 0.078
HA-EDA (D.S.: 50%)	2.882 ± 0.023

The isoelectric points for different types of polyampholytes are given in Table 4.3. As it is expected, the pI values increase with an increase in the degree of substitution due to the increase in amine groups, which are positively charged at lower pH levels. This is because a higher pH will be necessary in order to deprotonate sufficient amine groups in order to produce a net zero charge. The isoelectric point, at which the charges neutralize each other, should be at a higher pH in a polyampholyte with more amine groups than the other because of the higher degree of amination.

4.4. Turbidimetric pH Titrations

Turbidimetric pH titrations were conducted to obtain phase diagrams of different systems of polyampholytes with polyelectrolytes or proteins. Poly(styrene sulfonate) (PSS) and bovine serum albumin (BSA) were used for preliminary work. PSS, a strong anionic polyelectrolyte, was used to confirm the synthesis of polyampholytes besides characterization methods like ^{1}H-NMR and FTIR spectroscopy: The strong anionic polyelectrolyte of PSS is negatively charged at every pH. Thus, if we have a positively charged group on the HA-derived polyampholyte, the interaction should be able to be observed by turbidimetric titrations, because unmodified HA is a weak anionic polyelectrolyte. For these experiments, we used HA-ADH polyampholytes with 20% and 40 % degree of substitution, which were obtained at HA: ADH: EDC: HOBt ratios of 1: 20: 0.5: 0.5 and 1: 30: 4: 4, respectively.

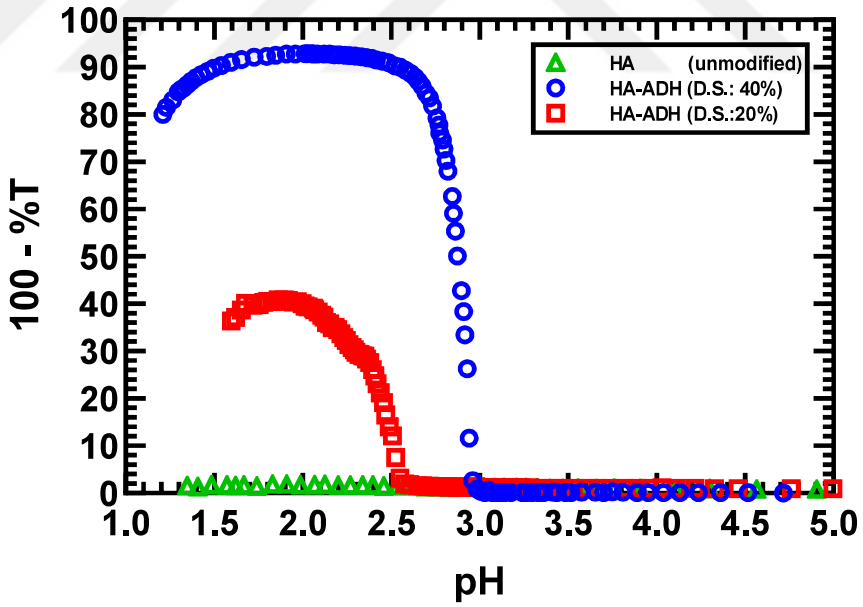

Figure 4.10. Turbidity (100-%T) vs. pH graph for the systems HA-ADH (40%), HA-ADH (20%), and HA after mixing with PSS with weight ratio Polymer: PSS – 5:1 (by weight) in salt-free medium. Concentrations after mixing was 0.83 mg/mL and 0.17 mg/mL for HA and HA-derived polyampholytes and PSS, respectively. Titrations were performed from basic to acidic pH.

In Figure 4.10, the maximum turbidity value belongs to the system containing the polyampholyte with higher degree of substitution, i.e. HA-ADH (40%). On the other hand, the HA-ADH polyampholyte with 20% degree of substitution could reach about half the turbidity value of the former one. As expected, there was no interaction between unmodified HA and PSS at the same condition due to electrostatic repulsion (Figure 4.10). Thus, we confirmed the synthesis of polyampholytes not only with using characterization methods but also with turbidimetric titration experiments.

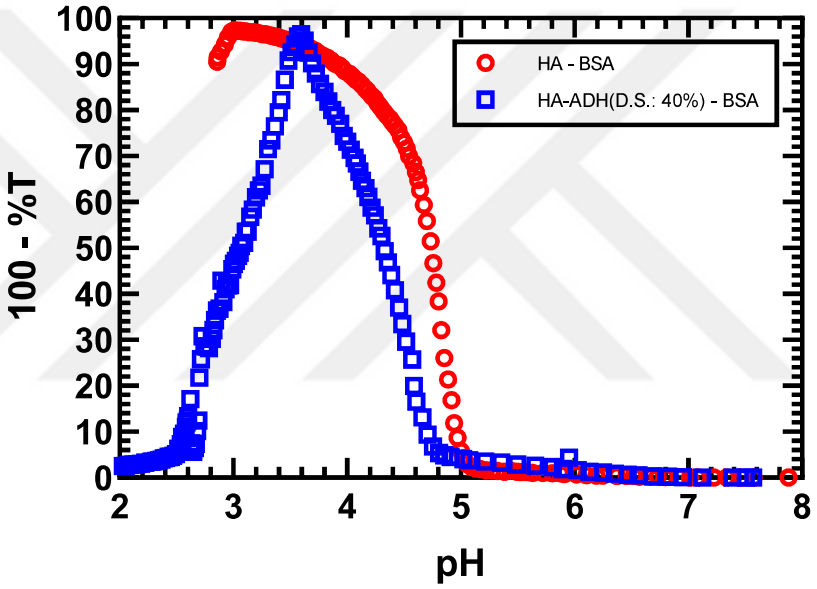

Figure 4.11. Turbidity (100-%T) vs. pH graph for the systems containing HA-ADH (40%) and HA by adding BSA with weight ratio of Polymer: BSA as 1:1 (by weight) in salt-free medium. Concentrations after mixing was 0.5 mg/mL for both polymers and BSA. Titrations were performed from basic to acidic pH.

In Figure 4.11, results from turbidimetric titrations of BSA mixtures with HA and HA-ADH (40%) are presented as a preliminary work regarding the complexation of PA with protein. The pH at which turbidity begins to increase is shifted to a more acidic pH, indicating stronger interactions with unmodified HA. Since the pI value of BSA is about pH 4.9 [59], the net charge of BSA is negative at pH values above the pI point. However, BSA has a positive charge patch at pH 5.6 in 0.005 M NaCl despite the net negative charge (Figure

4.12) [60]. Meanwhile, unmodified HA is more negatively charged than HA-ADH (D.S. 40%). Although a repulsion is expected between the more negatively charged HA and the overall net negative charge of BSA, the attraction between the HA and the charge patch of BSA overcomes the repulsion.

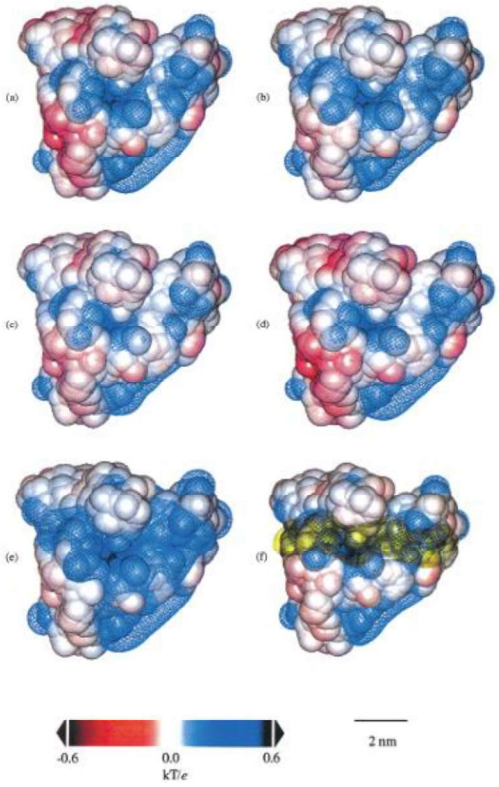

Figure 4.12. Surfaces with electrostatic potential shown by contours with +0.05 kT/e above 5 Å from the van der Waals surface. pH levels and ionic strength: (a) 0.005 M, 5.60 (pHc); (b) 0.15 M, 4.70 (pHc); (c) 0.15 M, 5.60; (d) 0.05 M, 7.65; (e) 0.10 M, 4.20 (pH); (f) identical to (b) with HA decamer superimposed on the proposed electrostatic binding site. (Adapted from Ref. [60] with permission from American Chemical Society)

Table 4.4.The optimum pH's and pI values of used enzymes.

Enzymes	Optimum pH	pI
alpha-Chymotrypsin (αCT)	7.8 [61]	8.76 [62]
Carbonic Anhydrase (CA)	7.5[63]	5.9[64]
Lysozyme (LYS)	6.24[65]	11[66]

In Table 4.4, the optimum pH's and pI values of the selected enzymes are given. The optimum pH of αCT is equal to 7.8 and its pI = 8.76 [61,62]. The optimum pH of CA is 7.5 and its pI = 5.9 [63,64]. The optimum pH for LYS is 6.24 and pI = 11 [65,66].The main aim of the turbidimetric pH titrations is to obtain the phase diagrams of different systems containing mixtures of synthesized polyampholytes and these enzymes at near optimum pH of the selected enzymes. When the pH < pI point, the net charge of the enzyme is positive and when pH > pI the net charge of the enzyme should be negative.

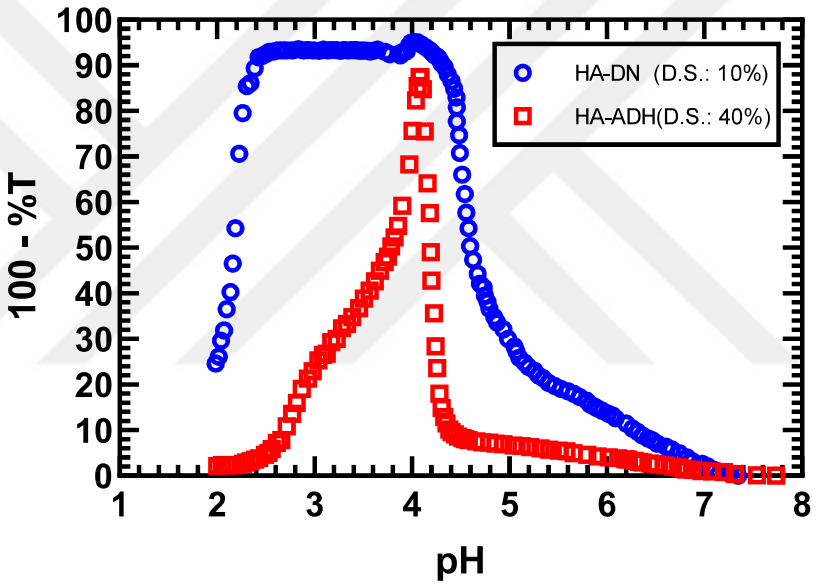

Figure 4.13. Turbidity (100-%T) vs. pH graph for mixtures of HA-ADH (40%) and HA-DN (10%) with CA at weight ratio of Polymer: CA as 1:3 in salt-free medium. Concentrations after mixing was at 0.1 mg/mL and 0.3 mg/mL for polymer and CA, respectively. Titrations were done from basic to acidic pH.

As seen from Figure 4.13, while doing the titration from basic to acidic pHs, the pH value where the turbidity starts to increase is more basic in HA-DN (10%) compared to HA-ADH (40%). Since the pI point of CA is 5.9, the enzyme has positive charge when pH < pI. The isoelectric points (pI) were determined to be 1.110 ± 0.015 for HA-DN (10%) and 2.401 ± 0.023 for HA-ADH (40%). Consequently, the polyampholytes has a net negative charge between their pI and pH 5.9, specifically between pH 1.1 and 5.9 for HA-DN (10%) and

between pH 2.4 and 5.9 for HA-ADH (40%). When the pH is smaller than 5.9, the PA should have a net negative charge. The higher turbidity values for HA-DN than HA-ADH (40%) is surprising since HA-DN (10%) has more negatively charged groups than HA-ADH (40%). For the future studies of enzymatic activity, it is desirable that the phase separation between PA and CA should be as close to pH 7.5, which is the optimum pH of CA. Although we tried other experimental conditions such as different weight ratios like 0.1 mg/mL : 0.5 mg/mL , 0.1 mg/mL : 0.1 mg/mL and 0.5 mg/mL : 0.5 mg/mL for HA-ADH(40%) : CA system (data not shown), we did not observe a strong interaction close to the enzyme optimum pH. As a result, further experiments with CA enzyme were only done with HA-DN (10%).

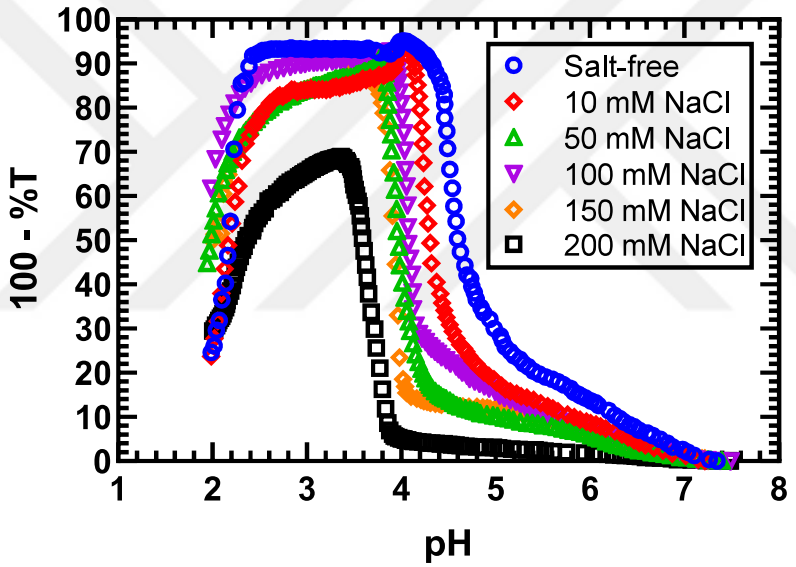

Figure 4.14. Turbidity (100-%T) vs. pH graph for the mixtures of HA-DN (10%) with CA at weight ratio of HA-DN (10%): CA as 1:3 in salt-free medium. Concentrations after mixing was 0.1 mg/mL and 0.3 mg/mL for HA-DN (10%) and CA, respectively. Titrations were done from basic to acidic pH.

To determine the effect of the salt concentration, a mixture containing 0.1 mg/mL HA-DN (10%) and 0.3 mg/mL CA was titrated with 0.1 N HCl, and turbidity was recorded at each pH.. As it can be seen from Figure 4.14, with the increase of salt concentration from salt-free (0 mM) to 200 mM NaCl, although there is no significant difference of the pH of the initial increase in turbidity, the steepness of the curve decreased. Also, at 200 mM NaCl,

the pH of the initial point of increase in turbidity value shifted from pH 7.22 to acidic one, pH 3.93 with respect to others.

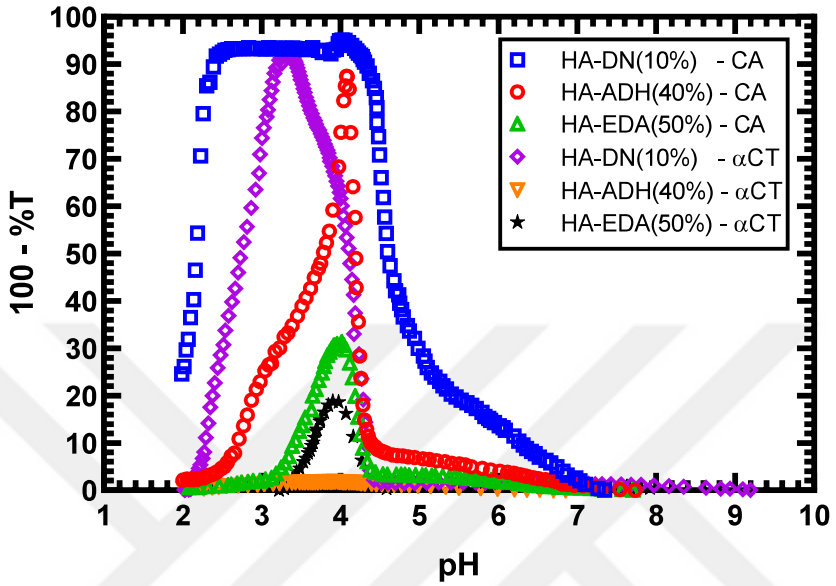

Figure 4.15. Turbidity (100-%T) vs. pH graph for mixtures of HA-DN (10%), HA-ADH (40%) and HA-EDA (50%) with CA and αCT at weight ratio of PA: Enzyme as 1:3 in salt-free medium. Polymer and enzyme concentrations after mixing were 0.1 mg/mL and 0.3 mg/mL, respectively. Titrations were done from basic to acidic pH.

Figure 4.15 shows the results of turbidimetric pH titrations between polyampholytes of HA-DN (10%), HA-ADH (40%) and HA-EDA (50%) and enzymes of CA and αCT.

In turbidimetric titration experiments for the mixture of CA with HA-ADH (40%) and HA-EDA (50%), phase separation started at around pH 4.4. At pH 4.4, the net charge of CA is positive since pH 4.4 < pI (CA) = 5.9. The polyampholytes, HA-ADH (40%) and HA-EDA (50%), were negatively charged at pH 4.4 since pH 4.4 > pI points of polyampholytes. Thus, the interaction at pH 4.4 was based on electrostatic attraction. On the other hand, for the mixture of HA-DN (10%)/CA, the interaction began at pH 7.3 where both macromolecules were negatively charged. These results might be explained by the presence of charge patches on CA. According to the charge patch mechanism, macromolecules with the same charge sign can still attract each when there is a charge patch with opposite charge

sign on one of the macromolecules. Unfortunately, we couldn't find a study in the literature that shows the electrostatic potential distribution of CA.

In all turbidimetric titration experiments with αCT, we would expect phase separation below pH 8.76, which is the pI of this enzyme. At pHs lower than 8.76, the net charge of the enzyme is positive while the polyampholytes are negatively charged. However, phase separation was not observed till pH was lowered to 4.4.

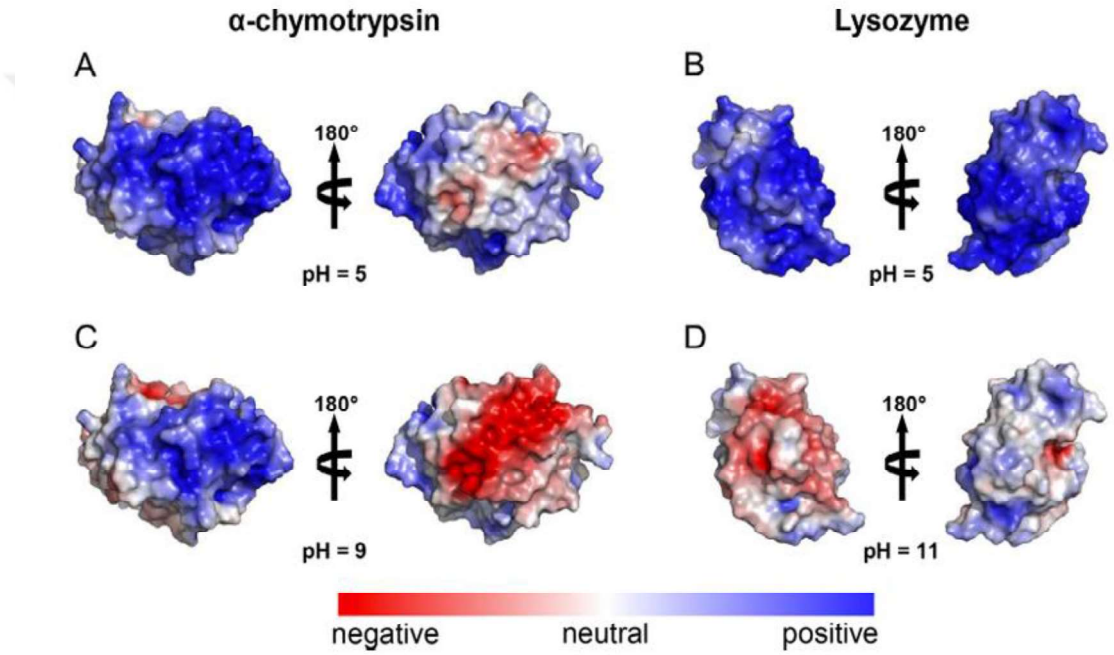

Figure 4.16. The illustration of surface charge distribution for alpha-chymotrypsin and lysozyme. (electrostatic potential:-5 keV, red; +5 keV, blue). A and B show the results for pH = 5, C and D show the results for pH ~ pI (pH = 9 for alpha-chymotrypsin and pH = 11 for lysozyme) (Adapted from Ref. [67] with permission from Elsevier)

This result can be explained by surface charge distribution of the proteins. Fernandez and coworkers [67] studied the surface charge distribution of αCT and LYS at pH = 5 and at their isoelectric points, i.e. pI = 9 for αCT and pI = 11 for LYS. In Figure 4.15C, the charges on the opposite sides showed an electrostatic bipolar distribution for αCT. Figure 4.15A and B shows the surface charge distribution of these enzymes at pH = 5, which is a pH lower than their pI values. As it can be seen in Figure 4.15A, one side of the αCT is strongly positive while the other side is neutral. On the other hand, both sides of LYS are seen

strongly positive in Figure 4.15B. Thus, the interaction between HA-derived polyampholytes and αCT might be challenging since the size of the negative region increases from pH 5 to 9, leading to a repulsion between the negative charges of the polyampholytes and the negatively charged region of αCT. Nevertheless, we decided to proceed the experiments with lysozyme since phase separation for the PA- αCT systems did not take place at the optimum pH of the αCT, i.e. around pH 7.8.

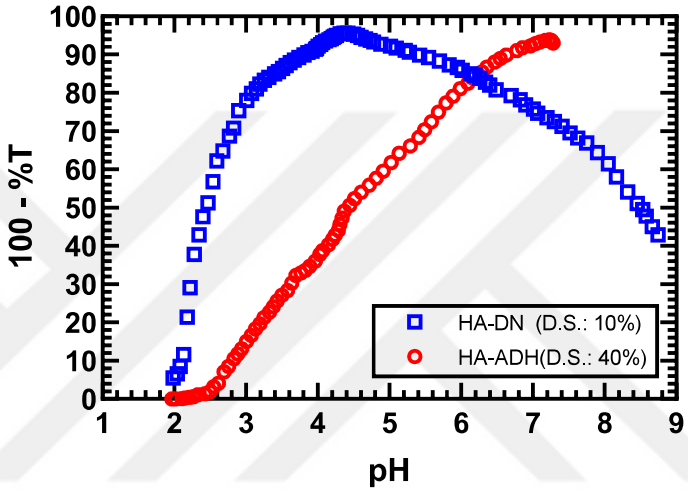

Figure 4.17. Turbidity (100-%T) vs. pH graph for the system of HA-DN (10%) and HA-ADH (40%) with LYS at weight ratio of PA: LYS as 1:3 in salt-free medium. Polymer and enzyme concentrations after mixing were 0.1 mg/mL and 0.3 mg/mL, respectively. Titrations were done from basic to acidic pH.

Results of the turbidimetric titrations for PA/LYS mixtures are presented in Figure 4.16. However, the obtained turbidity values were too high which could lead to precipitation. Because of this reason, the concentrations were reduced to half, i.e. 0.05 mg/mL for polyampholytes and 0.15 mg/mL for LYS (Figure 4.17).

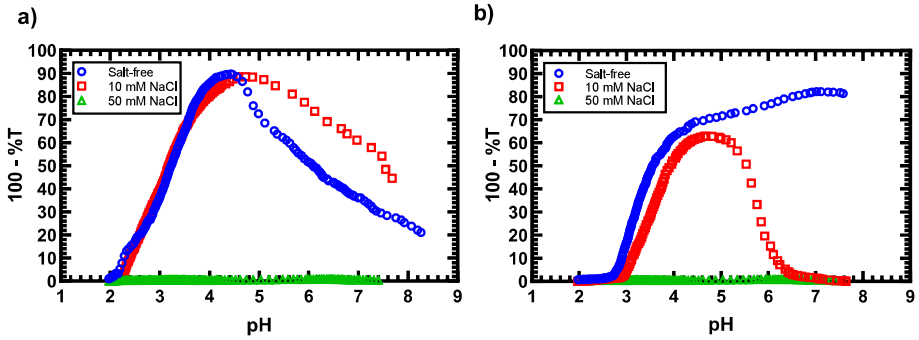

Figure 4.18. Turbidity (100-%T) vs. pH graph for the systems a) HA-DN (10%) (0.05 mg/mL) and LYS (0.15 mg/mL) b) HA-ADH (40%) (0.05 mg/mL) and LYS (0.15 mg/mL) at weight ratios of PA: LYS – 1:3 in salt-free medium. Titrations were done from basic to acidic pH.

As shown in Figure 4.17, positively charged LYS and negatively charged polyampholytes interacted with each other. Between salt-free solutions and 10 mM NaCl solutions, there was no drastic change in turbidities for the HA-DN (10%)/LYS system (Figure 4.17a) while the change was obvious for the HA-ADH (40%)/LYS system (Figure 4.17b). This result might be attributed to the fact that HA-DN (10%) has more negatively charged groups than HA-ADH (40%). On the other hand, with an increase of the salt concentration to 50 mM NaCl, no phase separation was observed for the PA/LYS system due to electrostatic screening of the charges.

5. CONCLUSION

In this study, polyampholytes based on hyaluronic acid with varying grafting ratios were synthesized using different types of diamines, and the interactions between polyampholytes and selected enzymes with different isoelectric points were examined.

Hyaluronic acid was modified to obtain zwitterionic biomacromolecules with using different types of diamines such as 1,4-Diaminobutane dihydrochloride (DN), adipic dihydrazide (ADH) and ethylenediamine dihydrochloride (EDA) via carbodiimide chemistry with EDC and NHS or HOBt. The structural characterization of polyampholytes were performed using ^{1}H-NMR spectroscopy by identifying the attached protons of diamines. In addition, the degree of substitutions was calculated by comparing the integration of newly introduced groups and the acetamido moiety of unmodified hyaluronic acid, which was used as an internal standard.

The formation of an amide bond was confirmed by the decrease in the intensity of carbonyl peak and an increase in amide II bond intensity relative to unmodified hyaluronic acid, as observed in the FTIR spectra. The zeta potential experiments were conducted for all types of polyampholytes and unmodified HA under various pH conditions. Furthermore, the isoelectric point (pI) of polyampholytes were determined by plotting the zeta potential measurements versus pH to detect the point where the line intersects the x-axis. It was observed that as the degree of substitution increased, the pI values also increased.

The turbidimetric-pH titration experiments were conducted to investigate the interactions between polyampholytes, with varying degree of substitutions, and enzymes with various isoelectric points, such as 8.76 for αCT, 5.9 for CA and 11 for LYS at the optimum pH's of selected enzymes, 7.8 for αCT, 7.5 for CA and 6.2 for LYS. The phase separation was observed when HA-DN (10%) and CA were used at 0.1 mg/mL and 0.3 mg/mL concentrations after mixing, respectively. In addition, the conditions of 0.05 mg/mL for HA-DN (10%) and HA-ADH (40%) with 0.15 mg/mL for LYS in salt-free and 10 mM NaCl solutions resulted in phase separation.

REFERENCES

1. Kayitmazer, A. B., A. F. Koksal and E. Kilic Iyilik, "Complex Coacervation of Hyaluronic Acid and Chitosan: Effects of pH, Ionic Strength, Charge Density, Chain Length and the Charge Ratio", *Soft Matter*, Vol. 11, No. 44, pp. 8605–8612, 2015.

2. Sing, C. E. and S. L. Perry, "Recent Progress in the Science of Complex Coacervation", *Soft Matter*, Vol. 16, No. 12, pp. 2885–2914, 2020.

3. Bungenberg De Jong, G., *Colloid Science*, vol II Reversible Systems, Elsevier, New York, 1949.

4. Pathak, J., E. Priyadarshini, K. Rawat and H. B. Bohidar, "Complex Coacervation in Charge Complementary Biopolymers: Electrostatic versus Surface Patch Binding", *Advances in Colloid and Interface Science*, Vol. 250, pp. 40–53, 2017.

5. Oparin, A. I., "The Origin of Life and the Origin of Enzymes", *Advances in Enzymology and Related Areas of Molecular Biology*, Vol. 27, pp. 347-380, 1965.

6. Ballesteros-Gómez, A., N. Caballero-Casero, S. García-Fonseca, L. Lunar and S. Rubio, "Multifunctional Vesicular Coacervates as Engineered Supramolecular Solvents for Wastewater Treatment", *Chemosphere*, Vol. 223, pp. 569–576, 2019.

7. Xu, Y., M. Mazzawi, K. Chen, L. Sun and P. L. Dubin, "Protein Purification by Polyelectrolyte Coacervation: Influence of Protein Charge Anisotropy on Selectivity", *Biomacromolecules*, Vol. 12, No. 5, pp. 1512–1522, 2011.

8. Yeo, Y., E. Bellas, W. Firestone, R. Langer and D. S. Kohane, "Complex Coacervates for Thermally Sensitive Controlled Release of Flavor Compounds", *Journal of Agricultural Food Chemistry*, Vol. 53, No. 19, pp. 7518–7525, 2005.

9. Huei, G. O. S., S. Muniyandy, T. Sathasivam, A. K. Veeramachineni and P. Janarthanan, "Iron Cross-Linked Carboxymethyl Cellulose-Gelatin Complex Coacervate Beads for Sustained Drug Delivery", *Chemical Papers*, Vol. 70, No. 2, pp. 243–252, 2015.

10. Zhou, L., H. Shi, Z. Li and C. He, "Recent Advances in Complex Coacervation Design from Macromolecular Assemblies and Emerging Applications", *Macromoecular Rapid Communications*, Vol. 41, No. 21, p. 2000149, 2020.

11. Mohanty, B. and H. B. Bohidar, "Systematic of Alcohol-Induced Simple Coacervation in Aqueous Gelatin Solutions", *Biomacromolecules*, Vol. 4, No. 4, pp. 1080–1086, 2003.

12. Wang, M. and Y. Wang, "Development of Surfactant Coacervation in Aqueous Solution", *Soft Matter*, Vol. 10, No. 40, pp. 7909–7919, 2014.

13. Veis, A., "A Review of the Early Development of the Thermodynamics of the Complex Coacervation Phase Separation", *Advances in Colloid and Interface Science*, Vol. 167, No. 1–2, pp. 2–11, 2011.

14. Martin, N., L. Tian, D. Spencer, A. Coutable-Pennarun, J. L. Ross Anderson and S. Mann, "Photoswitchable Phase Separation and Oligonucleotide Trafficking in DNA Coacervate Microdroplets", *Angewandte Chemie International Edition*, Vol. 58, No. 41, pp. 14594–14598, 2019.

15. Aumiller, W. M., B. W. Davis and C. D. Keating, "Phase Separation as a Possible Means of Nuclear Compartmentalization", *International Review Cell and Molecular Biology*, Vol. 307, pp. 109–149, 2014.

16. Wang, Y., "Effects of Salt on Polyelectrolyte-Micelle Coacervation", *Macromolecules*, Vol. 32, No. 21, pp. 7128–7134, 1999.

17. Du, X., P. L. Dubin, D. A. Hoagland and L. Sun, "Protein-Selective Coacervation with Hyaluronic Acid", *Biomacromolecules*, Vol. 15, No. 3, pp. 726–734, 2014.

18. Perro, A., L. Giraud, N. Coudon, S. Shanmugathasan, V. Lapeyre, B. Goudeau, J. P. Douliez and V. Ravaine, “Self-Coacervation of Ampholyte Polymer Chains as an Efficient Encapsulation Strategy”, *Journal of Colloid Interface Science*, Vol. 548, pp. 275–283, 2019.

19. Margossian, K. O., M. U. Brown, T. Emrick and M. Muthukumar, “Coacervation in Polyzwitterion-Polyelectrolyte Systems and Their Potential Applications for Gastrointestinal Drug Delivery Platforms”, *Nature Communications*, Vol. 13, No. 1, pp. 1–11, 2022.

20. Pickett, P. D., Y. Ma, N. D. Posey, M. Lueckheide and V. M. Prabhu, “Structure and Phase Behavior of Polyampholytes and Polyzwitterions”, *Macromolecular Engineering; Hadjichristidis N, Gnanou Y, Matyjaszewski K, Muthukumar M, Eds*, pp. 1-51, 2022.

21. Kudaibergenov, S. E., “Macromolecular Complexes of Polyampholytes”, *Pure and Applied Chemistry*, Vol. 92, No. 6, pp. 839–857, 2020.

22. Schroeder, M. E., K. M. Zurick, D. E. McGrath and M. T. Bernards, “Multifunctional Polyampholyte Hydrogels with Fouling Resistance and Protein Conjugation Capacity”, *Biomacromolecules*, Vol. 14, No. 9, pp. 3112–3122, 2013.

23. Cao, S., M. N. Barcellona, F. Pfeiffer, and M. T. Bernards, “Tunable Multifunctional Tissue Engineering Scaffolds Composed of Three-Component Polyampholyte Polymers”, *Journal of Applied Polymer Science*, Vol. 133, No. 40, p. 43985, 2016.

24. Barcellona, M. N., N. Johnson and M. T. Bernards, “Characterizing Drug Release from Nonfouling Polyampholyte Hydrogels”, *Langmuir*, Vol. 31, No. 49, pp. 13402–13409, 2015.

25. Gürer, F., R. Kargl, M. Bračič, D. Makuc, M. Thonhofer, J. Plavec, T. Mohan and K. S. Kleinschek, “Water-Based Carbodiimide Mediated Synthesis of Polysaccharide-Amino Acid Conjugates: Deprotection, Charge and Structural Analysis”, *Carbohydrate Polymers*, Vol. 267, p. 118226, 2021.

26. Madinya, J. J., L. W. Chang, S. L. Perry and C. E. Sing, “Sequence-Dependent Self-Coacervation in High Charge-Density Polyampholytes”, *Molecular Systems Design & Engineering*, Vol. 5, p. 632, 2020.

27. Kudaibergenov, S. E., “Advances in Synthetic Polyampholytes for Biotechnology and Medicine”, *Review Journal of Chemistry*, Vol. 10, No. 1, pp. 12–39, 2020.

28. Rumyantsev, A. M., N. E. Jackson and J. J. De Pablo, “Polyelectrolyte Complex Coacervates: Recent Developments and New Frontiers”, *Annual Review of Condensed Matter Physics*, Vol. 12.1, pp. 155–176, 2021.

29. Patrickios, C. S., L. R. Sharma, S. P. Armes and N. C. Billingham, “Precipitation of a Water-Soluble ABC Triblock Methacrylic Polyampholyte: Effects of Time, pH, Polymer Concentration, Salt Type and Concentration, and Presence of a Protein”, *Langmuir*, Vol. 15, No. 5, pp. 1613–1620, 1999.

30. Olov, N., H. Mirzadeh, R. Moradi, S. Rajabi, and S. Bagheri-Khoulenjani, “Shape Memory Injectable Cryogel Based on Carboxymethyl Chitosan/Gelatin for Minimally Invasive Tissue Engineering: In Vitro and in Vivo Assays”, *Journal of Biomedical Materials Research Part B: Applied Biomaterials*, Vol. 110, No. 11, pp. 2438–2451, 2022.

31. Avazverdi, E., H. Mirzadeh, M. Ehsani and S. Bagheri-Khoulenjani, “Polysaccharide-Based Polyampholyte Complex Formation: Investigating the Role of Intra-Chain Interactions”, *Carbohydrate Polymers*, Vol. 313, p. 120836, 2023.

32. Zhao, J., M. A. Johnson, R. Fisher, N. A. D. Burke and H. D. H. Stöver, “Synthetic Polyampholytes as Macromolecular Cryoprotective Agents”, *Langmuir*, Vol. 35, No. 5, pp. 1807–1817, 2019.

33. Fouillet, C. C. J., T. L. Greaves, J. F. Quinn, T. P. Davis, J. Adamcik, M-A. Sani, F. Separovic, C. J. Drummond, R. Mezzenga et al., “Copolyampholytes Produced from

RAFT Polymerization of Protic Ionic Liquids", *Macromolecules*, Vol. 50, No. 22, pp. 8965–8978, 2017.

34. Jaradat, D. M. M., "Thirteen Decades of Peptide Synthesis: Key Developments in Solid Phase Peptide Synthesis and Amide Bond Formation Utilized in Peptide Ligation", *Amino Acids*, Vol. 50, No. 1, pp. 39–68, 2017.

35. Hermanson, G. T., *Bioconjugate Techniques*, Academic Press, San Diego, 2013.

36. Pouyani, T. and G. D. Prestwich, "Functionalized Derivatives of Hyaluronic Acid Oligosaccharides: Drug Carriers and Novel Biomaterials", *Bioconjugate Chemistry*, Vol. 5, No. 4, pp. 339–347, 1994.

37. Nakajima, N. and Y. Ikada, "Mechanism of Amide Formation by Carbodiimide for Bioconjugation in Aqueous Media", *Bioconjugate Chemistry*, Vol. 6, No. 1, pp. 123–130, 1995.

38. Bulpitt, P. and D. Aeschlimann, "New Strategy for Chemical Modification of Hyaluronic Acid: Preparation of Functionalized Derivatives and Their Use in the Formation of Novel Biocompatible Hydrogels", *Journal of Biomedical Materials Research*, Vol. 47, No. 2, pp. 152-169, 1999.

39. Mojarradi, H., "Coupling of Substances Containing a Primary Amine to Hyaluronan via Carbodiimide-Mediated Amidation", 2010, http://urn.kb.se/resolve?urn=urn:nbn:se:uu:diva-149284, accessed on June 03, 2024.

40. Sánchez-Silva, L., N. Gutiérrez, P. Sánchez, A. Romero and J. L. Valverde, "Smart Microcapsules Containing Nonpolar Chemical Compounds and Carbon Nanofibers", *Chemical Engineering Journal*, Vol. 181–182, pp. 813–822, 2012.

41. Akpo, E., C. Colin, A. Perrin, J. Cambedouzou and D. Cornu, "Encapsulation of Active Substances in Natural Polymer Coatings", *Materials*, Vol. 17, Page 2774, Vol. 17, No. 11, p. 2774, 2024.

42. Řepka, D., A. Kurillová, Y. Murtaja and L. Lapčík, “Application of Physical-Chemical Approaches for Encapsulation of Active Substances in Pharmaceutical and Food Industries”, *Foods*, Vol. 12, Page 2189, Vol. 12, No. 11, p. 2189, 2023.

43. Ghosh, S. K., “Functional Coatings: By Polymer Microencapsulation”, *Functional Coatings: By Polymer Microencapsulation*, pp. 1–357, 2006.

44. Jahan, S., C. Doyle, A. Ghimire, D. Combita, J. K. Rainey, B. D. Wagner and M. Ahmed, “Elucidating the Role of Optical Activity of Polymers in Protein–Polymer Interactions”, *Polymers*, Vol. 16, No. 1, p. 65, 2024.

45. Zhao, M. and N. S. Zacharia, “Protein Encapsulation via Polyelectrolyte Complex Coacervation: Protection against Protein Denaturation”, *Journal of Chemical Physics*, Vol. 149, No. 16, p. 163326, 2018.

46. Perrin, D. D., “1042. Prediction of the Strengths of Some Organic Bases”, *Journal of Chemical Society*, No. 0, pp. 5590–5596, 1965.

47. Shafer, D. E., B. Toll, R. F. Schuman, B. L. Nelson, J. J. Mond and A. Lees, “Activation of Soluble Polysaccharides with 1-cyano-4-dimethylaminopyridinium Tetrafluoroborate (CDAP) for use in Protein-Polysaccharide Conjugate Vaccines and Immunological Reagents. II. Selective Crosslinking of Proteins to CDAP-Activated Polysaccharides,” *Vaccine*, vol. 18, no. 13, pp. 1273–1281, 2000.

48. Inman, J. K., “Thymus-Independent Antigens: The Preparation of Covalent, Hapten-Ficoll Conjugates,” *Journal of Immunology*, vol. 114, no. 2, pp. 704–709, 1975.

49. Tucker, I. M., J. C. W. Corbett, J. Fatkin, R. O. Jack, M. Kaszuba, B. MacCreath and F. McNeil-Watson, “Laser Doppler Electrophoresis Applied to Colloids and Surfaces”, *Current Opinion in Colloid & Interface Science*, Vol. 20, No. 4, pp. 215–226, 2015.

50. Lunardi, C. N., A. J. Gomes, F. S. Rocha, J. De Tommaso and G. S. Patience, "Experimental Methods in Chemical Engineering: Zeta Potential", *The Canadian Journal of Chemical Engineering*, Vol. 99, No. 3, pp. 627–639, 2020.

51. Danaei, M., M. Kalantari, M. Raji, H. S. Fekri, R. Saber, G. P. Asnani, S. M. Mortazavi, M. R. Mozafari, B. Rasti and A. Taheriazam, "Probing Nanoliposomes using Single Particle Analytical Techniques: Effect of Excipients, Solvents, Phase Transition and Zeta Potential", *Heliyon*, Vol. 4, p. e01088, 2018.

52. Corbett, J. C. W., M. T. Connah and K. Mattison, "Advances in the Measurement of Protein Mobility using Laser Doppler Electrophoresis – the Diffusion Barrier Technique", *Electrophoresis*, Vol. 32, No. 14, pp. 1787–1794, 2011.

53. Schanté, C. E., G. Zuber, C. Herlin and T. F. Vandamme, "Chemical Modifications of Hyaluronic Acid for the Synthesis of Derivatives for a Broad Range of Biomedical Applications", *Carbohydrate Polymers*, Vol. 85, No. 3, pp. 469–489, 2011.

54. Antunes, J. C., J. M. Oliveira, R. L. Reis, J. M. Soria, J. L. Gómez-Ribelles and J. F. Mano, "Novel Poly(L-lactic acid)/Hyaluronic Acid Macroporous Hybrid Scaffolds: Characterization and Assessment of Cytotoxicity", *Journal of Biomedical Materials Research Part A*, Vol. 94, pp. 856–869, 2010.

55. Pullicino, E., W. Zou, M. Gresil and C. Soutis, "The Effect of Shear Mixing Speed and Time on the Mechanical Properties of GNP/Epoxy Composites", *Applied Composite Materials*, Vol. 24, No. 2, pp. 301–311, 2017.

56. YuNong, C., H. ShihLan, L. MingYuan, L. YiTing, L. ChienHung, C. JiFeng, M. H. T. Nguyen, S. YungHsiang, C. ShangTing and W. LiChen., "Ameliorative Effect of Curcumin-Encapsulated Hyaluronic Acid-PLA Nanoparticles on Thioacetamide-Induced Murine Hepatic Fibrosis", *Internatiinal Journal of Environmental Research and Public Health*, Vol. 14, No. 1, p. 11, 2017.

57. Sizeland, K. H., K. A. Hofman, I. C. Hallett, D. E. Martin, J. Potgieter, N. M. Kirby, A. Hawley, S. T. Mudie, T. M. Ryan, R. G. Haverkamp and M. H. Cumming, “Nanostructure of Electrospun Collagen: Do Electrospun Collagen Fibers form Native Structures?”, *Materialia*, Vol. 3, pp. 90–96, 2018.

58. Mero, A. and M. Campisi, “Hyaluronic Acid Bioconjugates for the Delivery of Bioactive Molecules”, *Polymer*, Vol. 6, No. 2, pp. 346–369, 2014.

59. Kaibara, K., T. Okazaki, H. B. Bohidar and P. L. Dubin, “pH-Induced Coacervation in Complexes of Bovine Serum Albumin and Cationic Polyelectrolytes”, *Biomacromolecules*, Vol. 1, No. 1, pp. 100–107, 2000.

60. Grymonpré, K. R., B.A., Staggemeier, P. L. Dubin, & K.W. Mattison, “Identification by Integrated Computer Modeling and Light Scattering Studies of an Electrostatic Serum Albumin-Hyaluronic Acid Binding Site”, *Biomacromolecules*, Vol. *2*(2), pp.422-429.

61. Bender, M. L., G. E. Clement, F. J. Kezdy and H. D. A. Heck, “The Correlation of the pH (pD) Dependence and the Stepwise Mechanism of α-Chymotrypsin-Catalyzed Reactions”, *Journal of American Chemical Society*, Vol. 86, No. 18, pp. 3680–3690, 1964.

62. Ui, N., “Isoelectric Points and Conformation of Proteins: II. Isoelectric Focusing of α-Chymotrypsin and Its Inactive Derivative”, *Biochimica et Biophysica Acta - Protein Structure*, Vol. 229, No. 3, pp. 582–589, 1971.

63. Demir, Y., N. Demir, H. Nadaroglu and E. Bakan, “Purification and Characterization of Carbonic Anhydrase from Bovine Erythrocyte Plasma Membrane”, *Preparative Biochemistry & Biotechnology*, Vol. 30, No. 1, pp. 49–59, 2000.

64. Tulp, A., M. Fernandez-Borja, D. Verwoerd and J. Neefjes, “High-Resolution Density Gradient Electrophoresis of Subcellular Organelles and Proteins under Nondenaturing Conditions”, *Electrophoresis*, Vol. 19, No. 8–9, pp. 1288–1293, 1998.

65. Cerón, A. A., L. Nascife, S. Norte, S. A. Costa, J. H. O. do Nascimento, F. D. P. Morisso, J. Baruque-Ramos, R. C. Oliveira and S. M. Costa, “Synthesis of Chitosan-Lysozyme Microspheres, Physicochemical Characterization, Enzymatic and Antimicrobial Activity”, *International Journal of Biological Macromolecules*, Vol. 185, pp. 572–581, 2021.

66. Rohani, M. M. and A. L. Zydney, “Effect of Surface Charge Distribution on Protein Transport through Semipermeable Ultrafiltration Membranes”, *Jornal of Membrane Science*, Vol. 337, No. 1–2, pp. 324–331, 2009.

67. Tournois, M., S. Mathé, I. André, J. Esque and M. A. Fernández, “Surface Charge Distribution: a Key Parameter for Understanding Protein Behavior in Chromatographic Processes”, *Journal of Chromatography A*, Vol. 1648, p. 462151, 2021.

APPENDIX A: SUPPLEMENTARY DATA

Appendix A contains the trials of the experiments conducted.

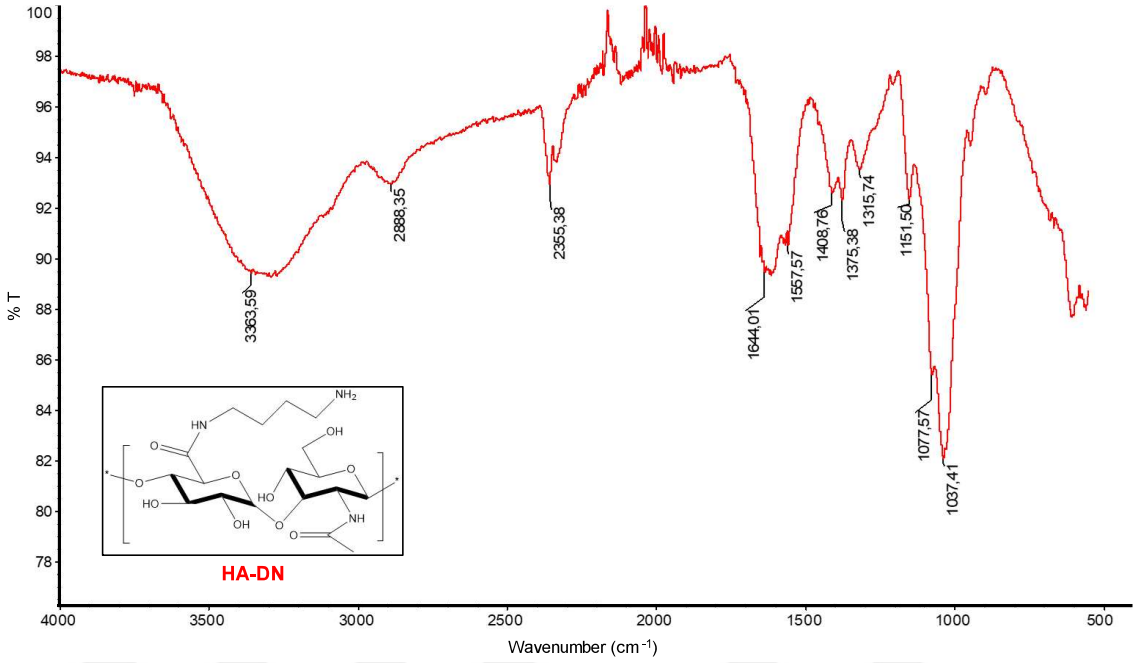

Figure A. 1. FTIR spectrum of HA-DN polyampholyte.

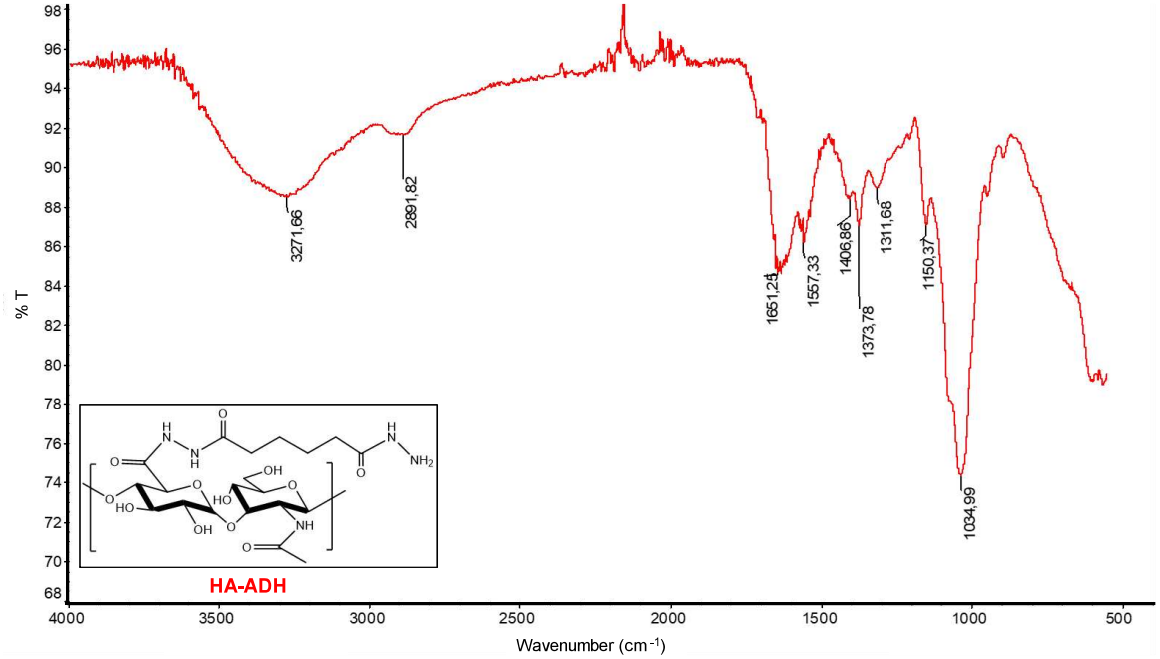

Figure A. 2. FTIR spectrum of HA-ADH polyampholyte.

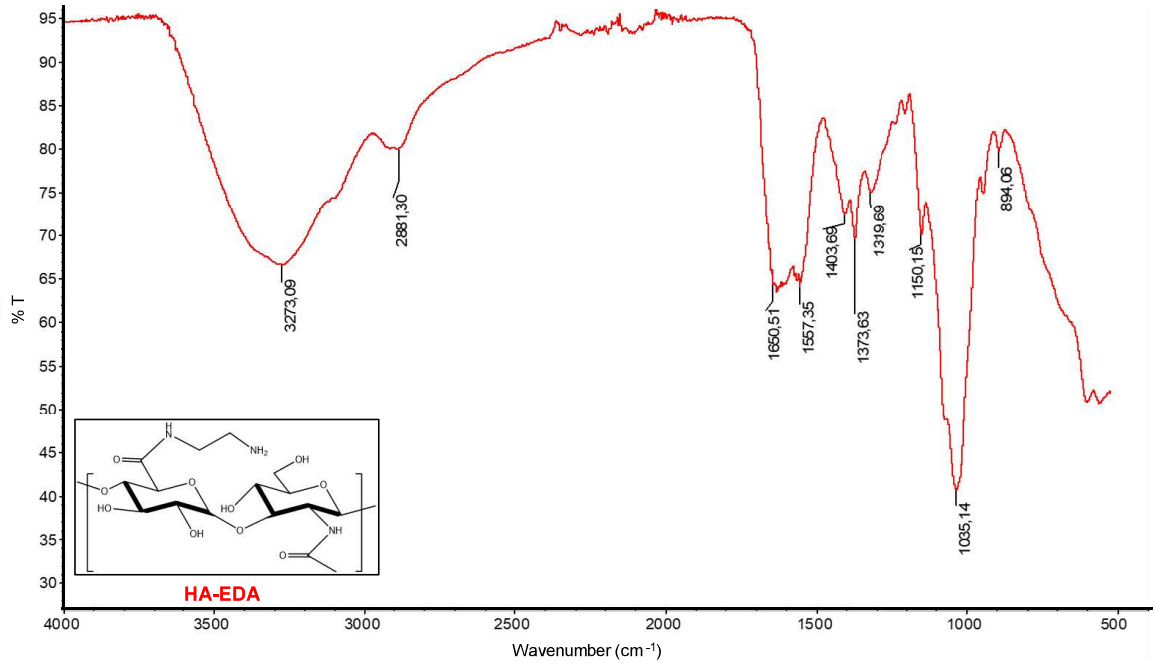

Figure A. 3. FTIR spectrum of HA-EDA polyampholyte.

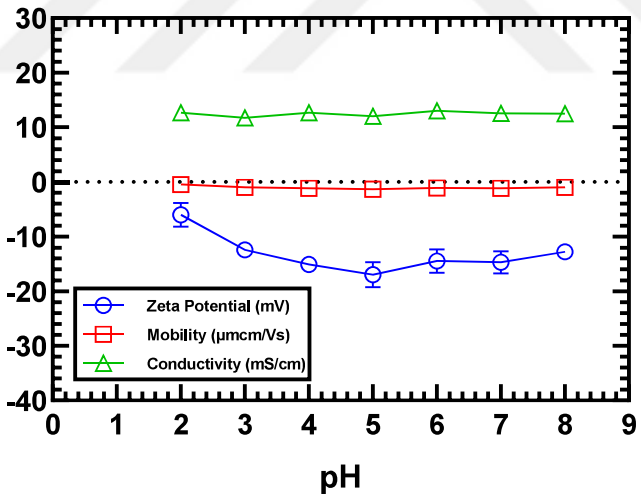

Figure A. 4. Zeta potential, mobility and conductivity measurements at different pHs for unmodified HA.

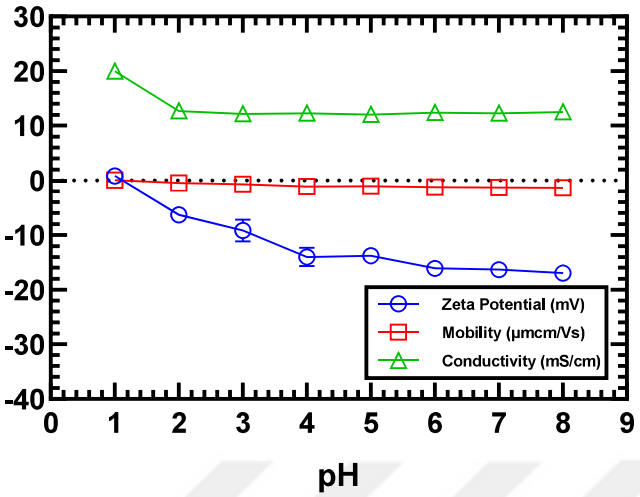

Figure A. 5. Zeta potential, mobility and conductivity measurements at different pHs for HA-DN polyampholyte.

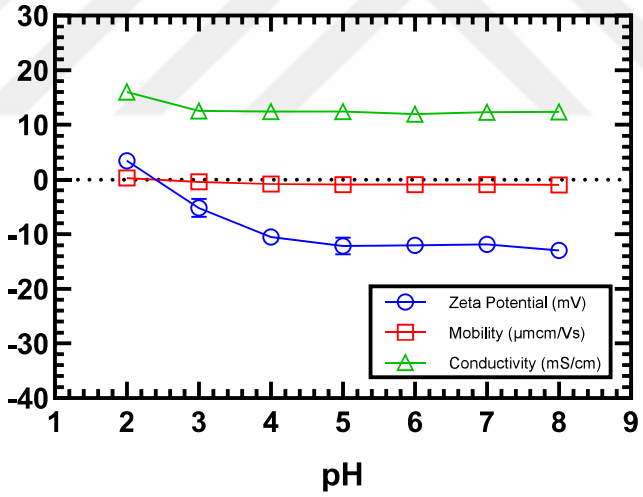

Figure A. 6. Zeta potential, mobility and conductivity measurements at different pHs for HA-ADH polyampholyte.

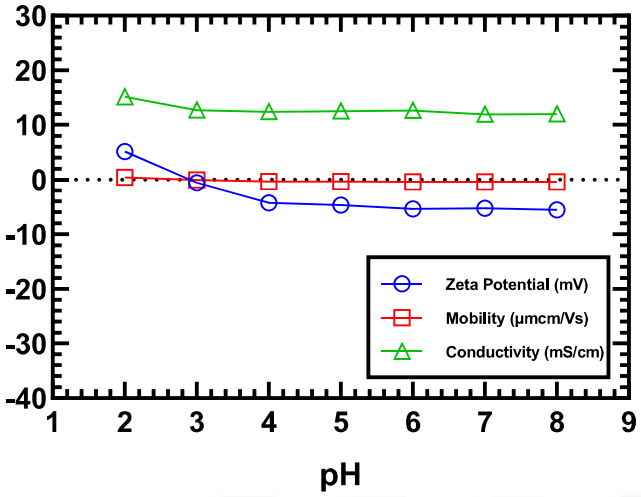

Figure A. 7. Zeta potential, mobility and conductivity measurements at different pHs for HA-EDA polyampholyte.

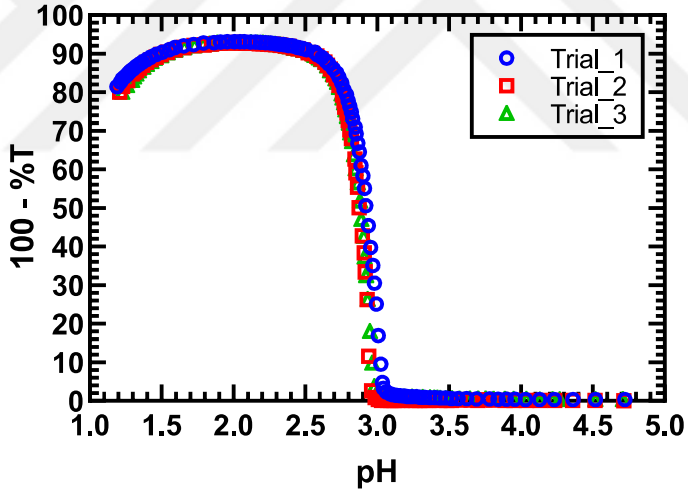

Figure A. 8. Turbidity (100-%T) vs. pH graph for the system containing HA-ADH (40%) and PSS weight ratio PA: PSS – 5:1 in salt-free medium. Concentrations after mixing were 0.83 mg/mL and 0.17 mg/mL for HA-ADH (40%) and PSS, respectively. Titrations were done from basic to acidic pH.

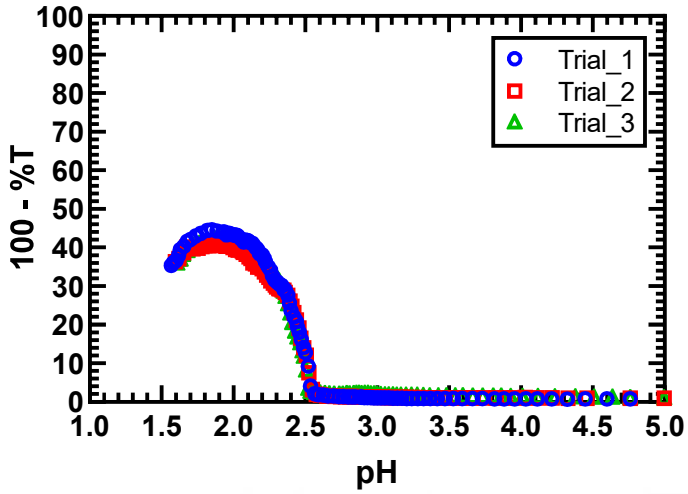

Figure A. 9. Turbidity(100-%T) vs. pH graph for the systems HA-ADH (20%) with PSS at weight ratio PA: PSS – 5:1 in salt-free medium. Concentrations after mixing were 0.83 mg/mL and 0.17 mg/mL for HA-ADH (20%) and PSS, respectively. Titrations were done from basic to acidic pH.

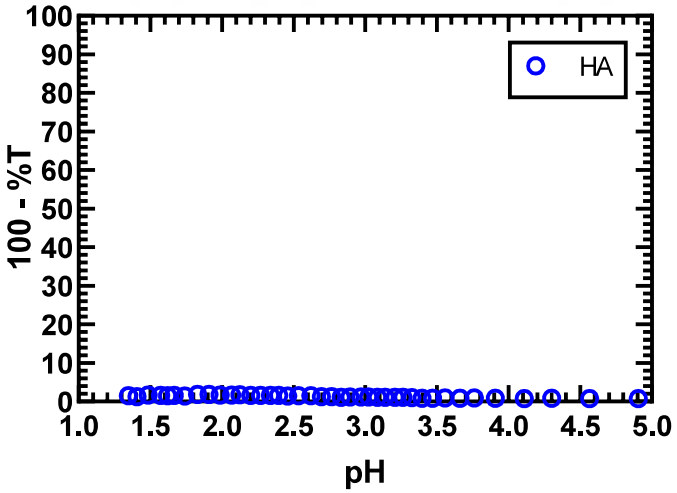

Figure A. 10. Turbidity(100-%T) vs. pH graph for the systems HA with PSS at weight ratio HA: PSS – 5:1 in salt-free medium. Concentrations after mixing were 0.83 mg/mL and 0.17 mg/mL for HA and PSS, respectively. Titrations were done from basic to acidic pH.

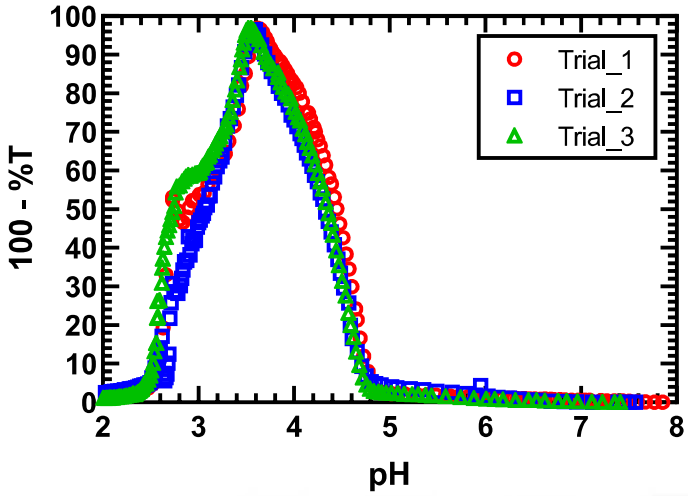

Figure A. 11. Turbidity(100-%T) vs. pH graph for the systems HA-ADH (40%) with BSA at weight ratio Polymer: BSA – 1:1 in salt-free medium. Concentrations after mixing were 0.5 mg/mL for both HA-ADH (40%) and BSA. Titrations were done from basic to acidic pH.

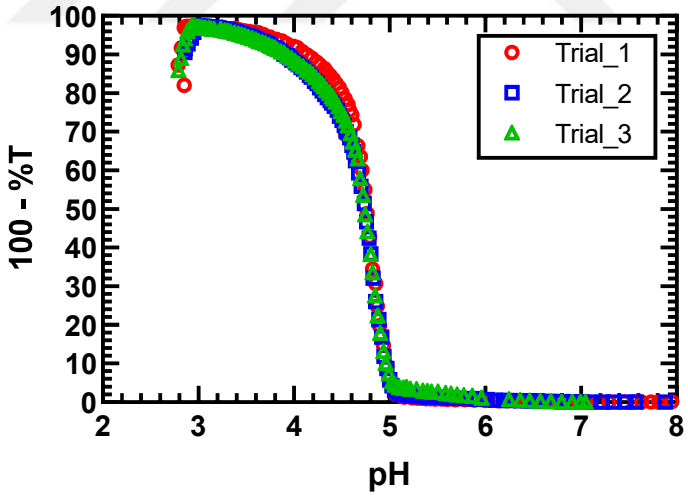

Figure A. 12. Turbidity(100-%T) vs. pH graph for the systems HA with BSA at weight ratio Polymer : BSA – 1:1 in salt-free medium. Concentrations after mixing were 0.5 mg/mL for both HA and BSA. Titrations were done from basic to acidic pH.

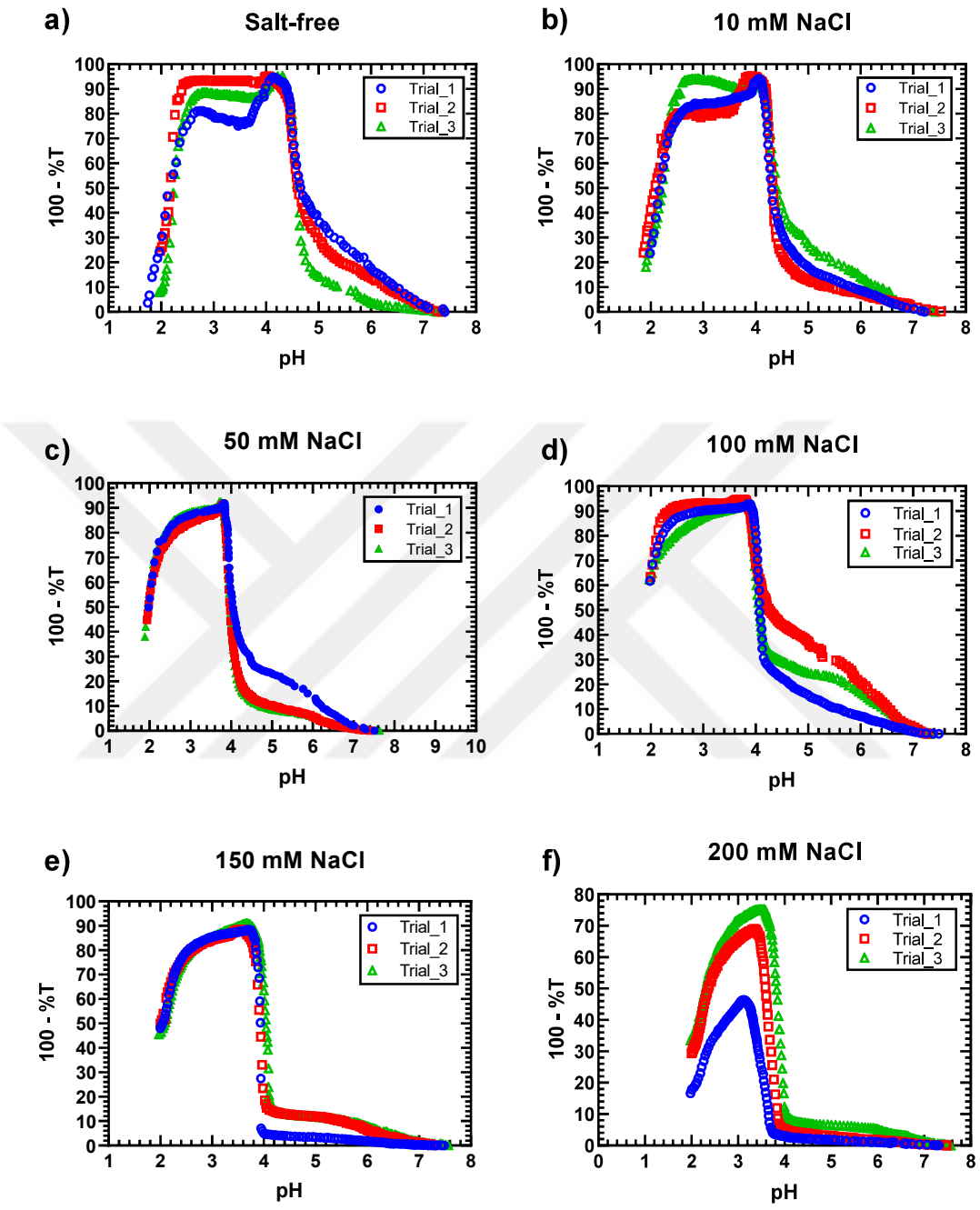

Figure A. 13. Turbidimetric-pH titration graphs for HA-DN (10%)/CA system. at different salt concentrations: (a) salt-free, (b)10 mM NaCl, (c) 50 mM NaCl, (d) 100 mM NaCl, (e) 150 mM NaCl, and (f) 200 mM NaCl. HA-DN and CA concentrations were 0.1 mg/mL and 0.3 mg/mL, respectively. Titrations were done from basic to acidic pH.

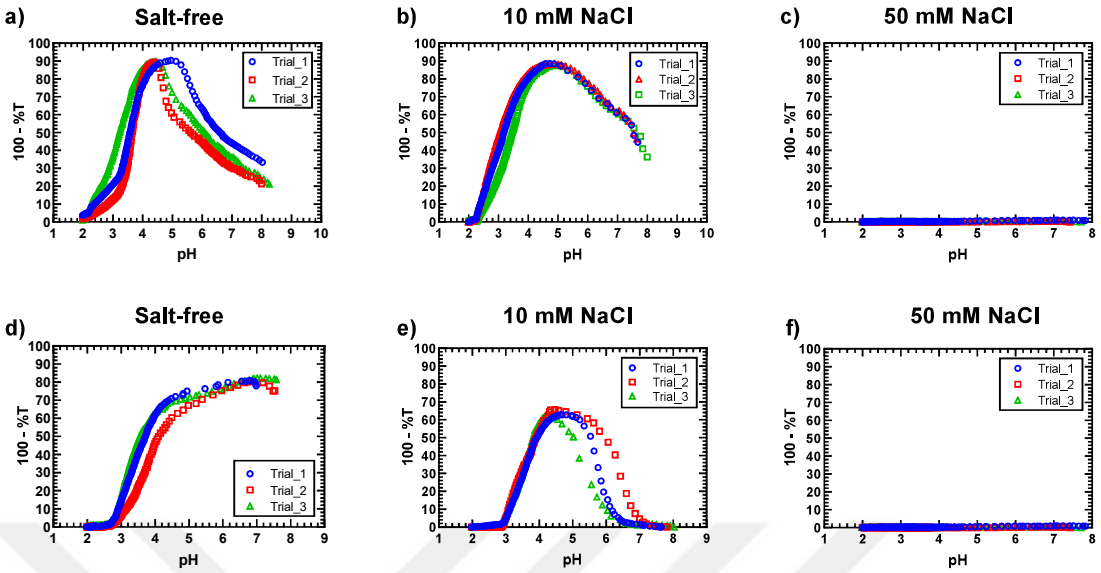

Figure A. 14. Turbidimetric-pH titration graphs. (a-c) HA-DN (10%) (0.05 mg/mL)/ LYS(0.15 mg/mL) system. (d-f) HA-ADH (40%) (0.05 mg/mL)/LYS (0.15 mg/mL) system. Titrations were done from basic to acidic pH.

APPENDIX B: COPYRIGHT LICENCES

Appendix B includes the permissions for the figures cited.

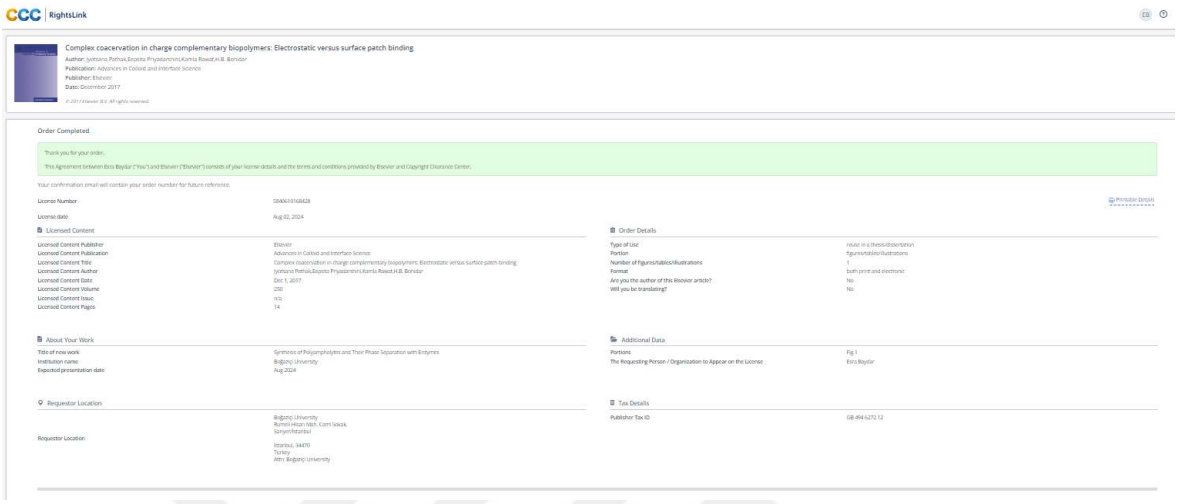

Figure B. 1. Permission of Ref. [4] from Elsevier

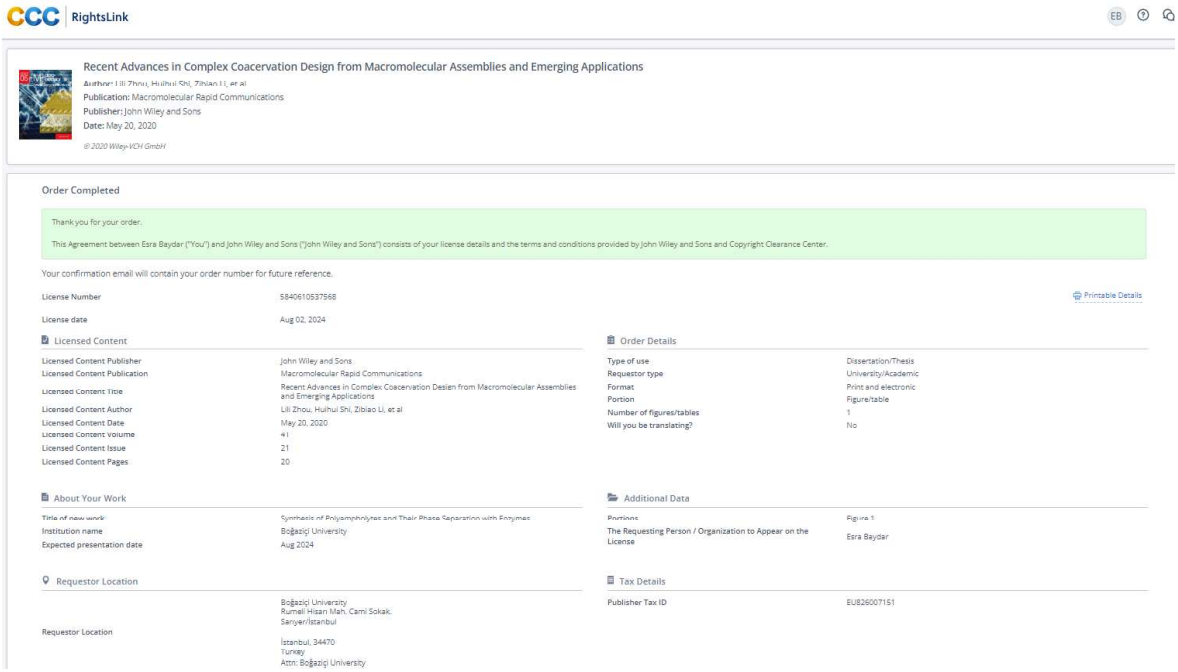

Figure B. 2. Permission of Ref. [10] from John Wiley and Sons

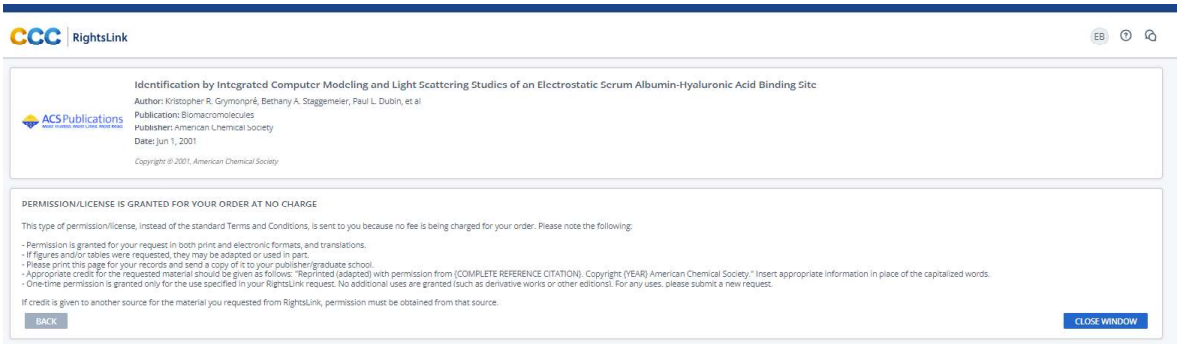

Figure B. 3. Permission of Ref. [60] from American Chemical Society

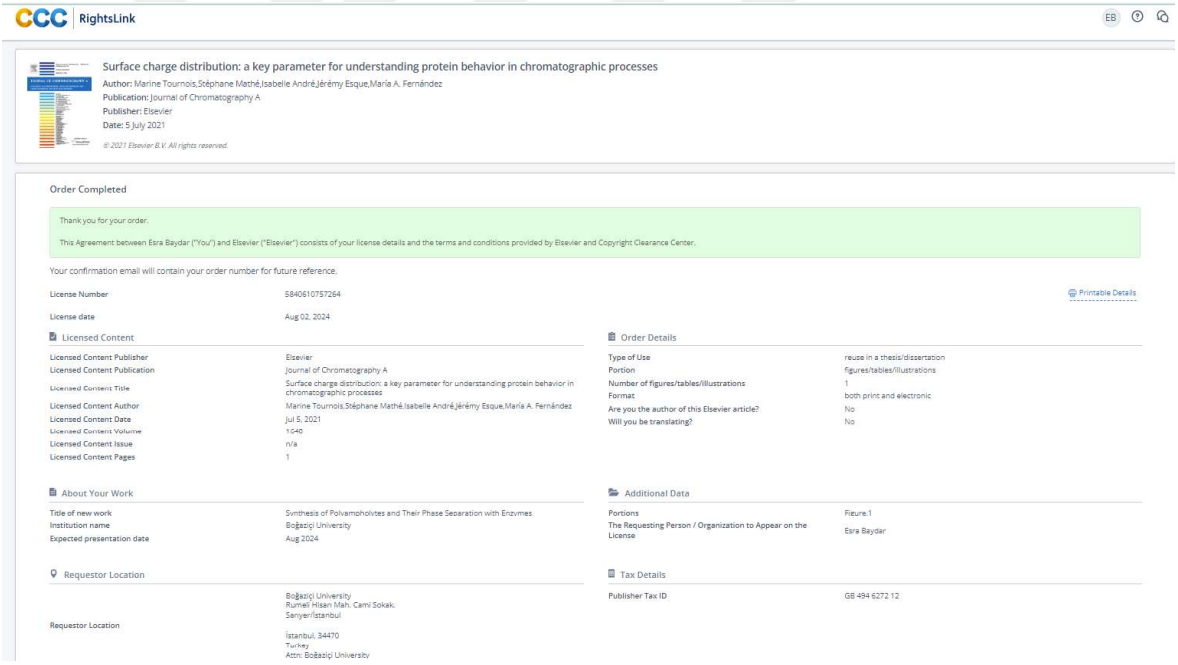

Figure B. 4. Permission of Ref. [67] from Elsevier